



LOS ANGELES - LAS VEGAS SECTION
JULY, 2023

SHAPING THE FUTURE OF AEROSPACE



Vaughan

AMERICAN INSTITUTE of AERONAUTICS and ASTRONAUTICS
LOS ANGELES - LAS VEGAS SECTION



4

(July 22) AIAA LA-LV Section
Outreach Pop-up Tent and Booth in
Aerospace Summer Games 2023



14

Paid Donation Advertisement
Buzz On Mars - 2017 and 2023
(Artist: James Vaughan)



21

Owens Valley Radio Observatory tour
(Photo Essay by Ms. Michelle Evans)



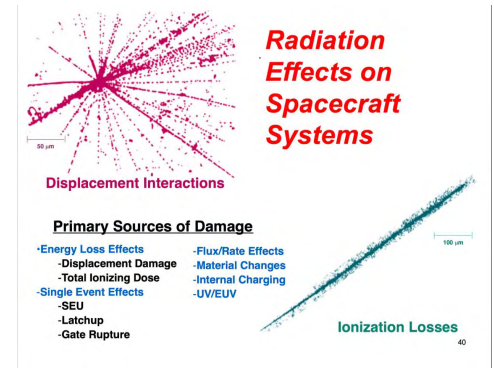
15

NGC 663
(by Dr. David H. Levy)



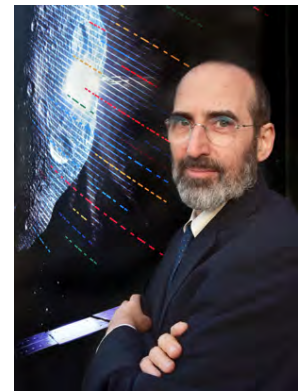
28

AIAA LA-LV Aero Alumni Meeting
(July 12)



10

(July 15) Spacecraft Environment Effects
and Mitigation Methods, #1,
with Dr. Henry B. Garrett



17

What Is a Philosopher Doing in
Planetary Defense?
(by Prof. Joel Marks)



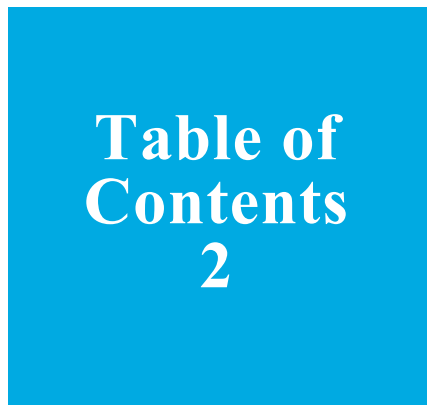
29

Falcon 9 Launch on July 19
(Photo Gallery by Ms. Michelle Evans)



32

Targeting Interplanetary Departures & Arrivals
From The Moon (by Mr. Dan Adamo)



56

AIAA Journals



58

AIAA National 2023 Fall Course Catalog
Released



62

Announcement:
AIAA Email notices frequency adjustment



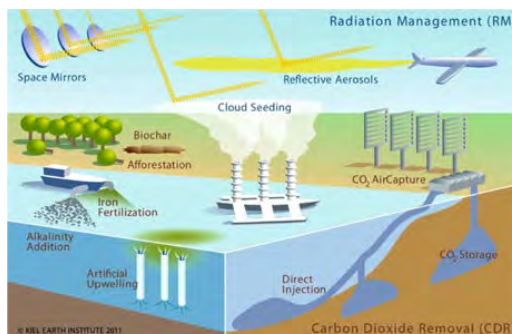
63

Announcement
AIAA LA-LV Section Career Resources



64

Aerospace News Digest



65

Upcoming AIAA / LA-LV Events



American Institute of Aeronautics and Astronautics
Los Angeles - Las Vegas Section

Newsletter

(July 22) AIAA LA-LV Section Outreach Pop-up Tent and Booth in Aerospace Summer Games 2023

(Photos Only) (<https://www.aiaa-lalv.org/blogs/2023-blogs/2023-july/2023-july-22>)



(Upper Left) Luis Cuevas (in black T-shirt, Young Professional Chair) and Ian Clavio (in blue T-shirt, Education / Collegiate Chair) talked to the visitors at the AIAA LA-LV Section Tent / Booth. (Upper Right) Ian Clavio (standing) and Luis Cuevas (sitting). (Bottom) A snapshot on the Dockweiler Beach during the Aerospace Summer Games 2023 (Organizer this year: SpaceX).

Disclaimer: The views of the speakers do not represent the views of AIAA or the AIAA Los Angeles-Las Vegas Section. Advertising space is available in the AIAA Los Angeles-Las Vegas Newsletter: Business card, quarter page, half page, and full page, non-AIAA LA-LV business/issues

The newsletter has over approx. 9,000 subscribers, and has been growing.

To inquire about purchasing advertising, email Newsletter Editor at editor.aiaalav@gmail.com, or, editor-newsletter@aiaa-lalv.org



American Institute of Aeronautics and Astronautics
Los Angeles - Las Vegas Section

aiaa-lalv.org | aiaa-lasvegas.org
engage.aiaa.org/losangeles-lasvegas

(July 22) AIAA LA-LV Section Outreach Pop-up Tent and Booth in Aerospace Summer Games 2023 *(Photos Only)*



Many visitors stopped by and engaged in interesting conversations. It was great fun. And people had small reunions at the Section tent, too!

(July 22) AIAA LA-LV Section Outreach Pop-up Tent and Booth in Aerospace Summer Games 2023 *(Photos Only)*



AIAA promotional items were handed out, with the membership brochures, while membership benefits were explained.

(July 22) AIAA LA-LV Section Outreach Pop-up Tent and Booth in Aerospace Summer Games 2023 *(Photos Only)*



Some high school students, like those 2 in the photos here, got interested in AIAA, and learned more about AIAA, and the free AIAA High School Membership. They happily picked up the AIAA bags and other promotion items and brochures / flyers.

(July 22) AIAA LA-LV Section Outreach Pop-up Tent and Booth in Aerospace Summer Games 2023 *(Photos Only)*



It was estimated 3,000 - 5,000 people in the area participating or watching games there. Luis, Ian, and Ken, did the best to network or help people network together, and know more AIAA as an organization / institute, and AIAA membership, sharing experiences.

(July 22) AIAA LA-LV Section Outreach Pop-up Tent and Booth in Aerospace Summer Games 2023 *(Photos Only)*



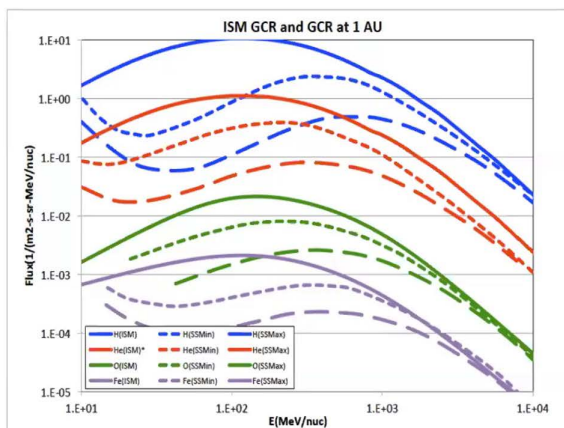
Many visitors were very interested in the displays, models, brochures, conversations, networking, asking good questions and making connections. Luis and Ian, with great smiles and professional attitude, attracted many visitors, also with smiles, making it a memorable and fun experience for all. See you next year again!

(2023 July 15) Spacecraft Environment Effects and Mitigation Methods, #1, with Dr. Henry B. Garrett (Screenshots & Photos Only)

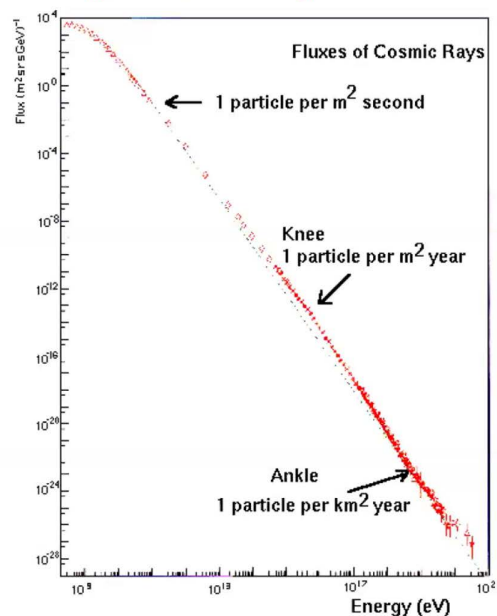
<https://www.aiaa-lalv.org/blogs/2023-blogs/2023-july/2023-july-15>

Spacecraft Environment Interactions

1 AU Cosmic Ray Nuclear Species Spectra

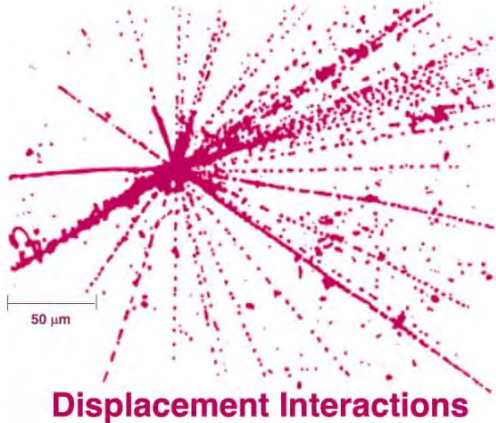


GCR ions at 1 AU for SSMin and SSMMax and in Interstellar Space (R. Mewaldt and others).



Attendees gathered in person and on-line, for the exciting and fun lecture by Dr. Henry Garrett, on spacecraft environment interactions, radiation nuclear species in space, space weather etc. This is part 1 of a series of lectures by Dr. Garrett. More will be available soon.

(2023 July 15) Spacecraft Environment Effects and Mitigation Methods, #1, with Dr. Henry B. Garrett *(Screenshots & Photos Only)*



Radiation Effects on Spacecraft Systems

(Left) Dr. Garrett explained various types of radiation effects on spacecraft systems, and the primary sources of damage for those interactions and losses.

Primary Sources of Damage

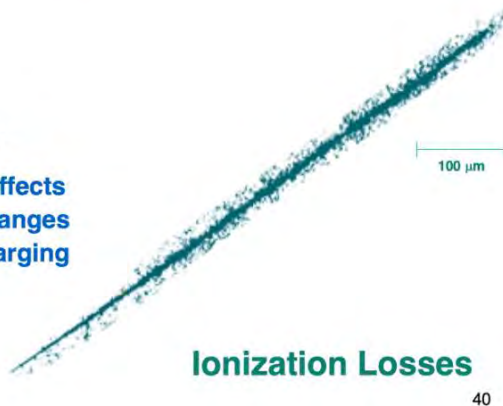
•Energy Loss Effects

- Displacement Damage
- Total Ionizing Dose

•Single Event Effects

- SEU
- Latchup
- Gate Rupture

- Flux/Rate Effects
- Material Changes
- Internal Charging
- UV/EUV

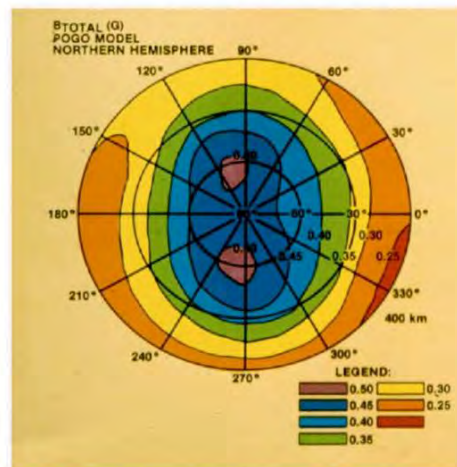


Spacecraft Environment Interactions

THE MAGNETIC FIELD OF THE EARTH

MAGNETIC INTENSITY AT THE EARTH'S SURFACE

THE SOUTH ATLANTIC ANOMALY



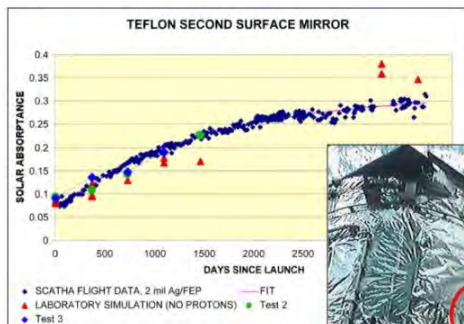
(Right) Dr. Garrett also elucidated the importance of the Earth's magnetic field at the surface, and its effects on the radiation environment, space weather, including the interesting case of the well-known South Atlantic Anomaly.



35

(2023 July 15) Spacecraft Environment Effects and Mitigation Methods, #1, with Dr. Henry B. Garrett *(Screenshots & Photos Only)*

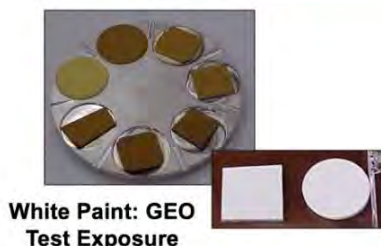
Spacecraft Environment Interactions



**Silver Teflon:
Flight Data**



**Tedlar: 3-4 Yrs GEO
Test Exposure**



**White Paint: GEO
Test Exposure**

Radiation Effects on Materials

Materials suffer from UV/EUV and particle radiation (Grads on surfaces!) through changes in:

- Dimensions
- Tensile strength
- Conductivity
- Transmission
- Reflectance
- Decomposition

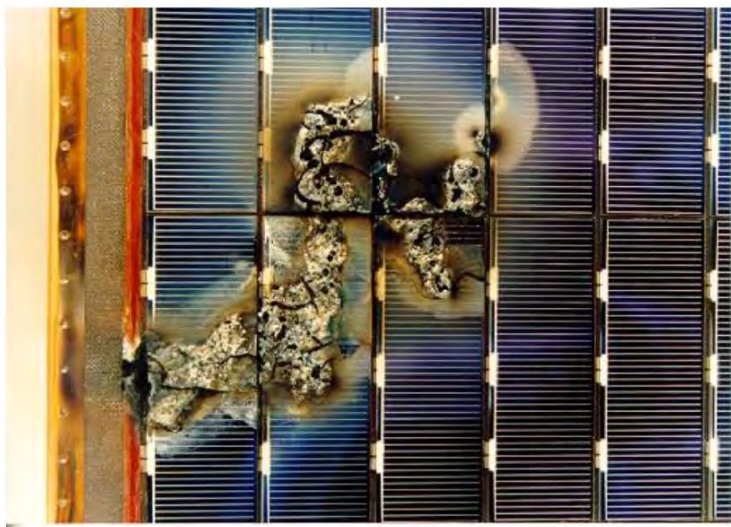
Adapted from Meshishnek et al., 2004
Courtesy of the Aerospace Corporation

64

(Left) The speaker explained the effects of radiation on materials, like the UV/EUV and particle radiations, through changes in dimensions, tensile strengths, conductivities etc.

Spacecraft Environment Interactions

Results of a Discharge on the European Eureka Solar Array



(Right) Example of the effects of spacecraft surface charging on a solar array sample.

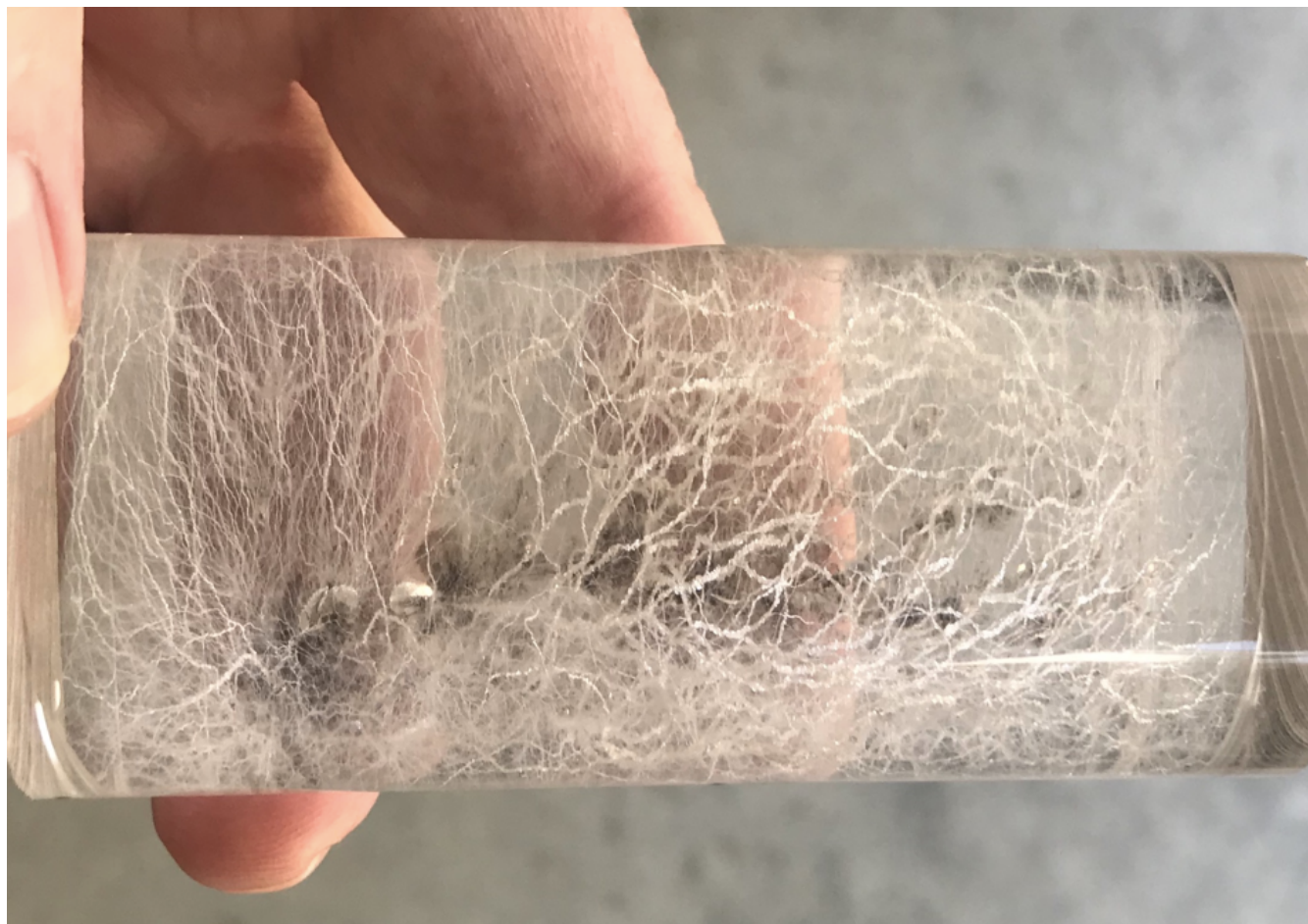
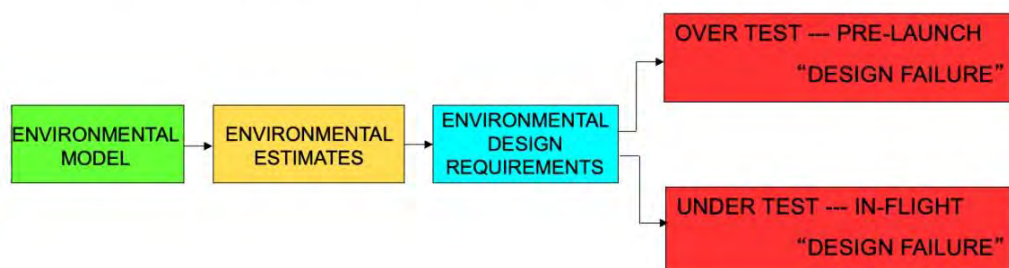
94

(2023 July 15) Spacecraft Environment Effects and Mitigation Methods, #1, with Dr. Henry B. Garrett *(Screenshots & Photos Only)*

Spacecraft Environment Interactions

(Left) Dr. Garrett pointed out the balance between under test and over test, and the impact of space environment and testing on spacecraft failures.

Impact Of Space Environment and Testing On Spacecraft Failures



(Above) Example of an internal electrostatic discharge in a cable illustrating a Lichtenberg arc breakdown.

Donation / Paid Advertisement

Cover Page: USAF C-5 'Galaxy' (Lockheed); emerging from storm."
Artist: Mr. James Vaughan



Here is the link if you are interested in having your own copies of the artwork, ordering a cover or page from the magazine/newsletters; as a fine art print or coffee cup etc.

<https://fineartamerica.com/featured/c-5-galaxy-emerging-from-storm-james-vaughan.html?product=art-print>

James Vaughan was born in 1955 and grew-up in an idyllic Ohio small town. His father was head of research for Goodyear and his mother was an artist and poet.

Studying history and politics he gained a degree in photography and journalism. He worked in the Chicago advertising industry for three decades.

Now, returned to his small town roots in the Midwest; he has built new studio facilities and earned world-wide attention for his commissioned artwork of aerospace, defense and science subjects. His work has been used by government, magazines, television, advertising and a myriad of technical publications and presentations. The US Postal Service has recently used his art of the James Webb Space Telescope for a popular first-class 'forever stamp'.

James Vaughan's unique skills and experience; from the start of the Space Age to today's programs for the Moon and Mars - give his illustrations a feel of adventure and higher purpose. Modern day mythology which calls to the heart and essence of our journey to the stars.

EMAIL: james@jamesvaughanphotoillus.com
PHONE: (330) 678-9010

MAIN PORTFOLIO/ GALLERY:
<http://www.jamesvaughanphotoillus.com/>

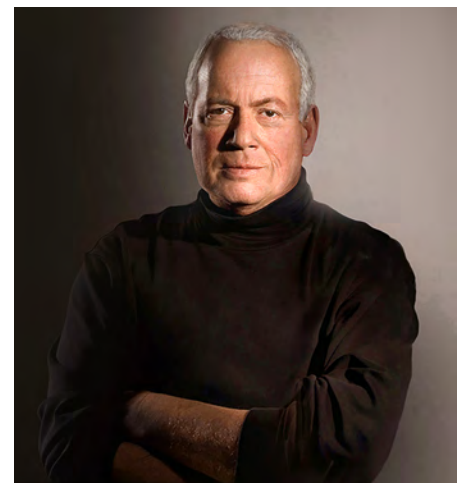
ARTWORK ON VIDEO:
<https://vimeo.com/showcase/5136121>

PORTFOLIO:
<https://www.flickr.com/photos/jamesvaughanphoto/>

ARTWORK 'MAGAZINES'- ISSUU
<https://issuu.com/jamesvaughanphoto>

PRINTS, POSTERS misc.

<https://fineartamerica.com/profiles/3-james-vaughan>



NGC 663

by Dr. David H. Levy, Comet and Asteroid Hunter, Co-Discoverer, Shoemaker-Levy 9 (2023 August article)



Photo credit:
Dominique and Gerald MacKenzie

One of the first astronomy books I ever read was John Benson Sidgwick's *Introducing Astronomy*. Thew book was published in 1959, a year after his death. In it was a large section in which each constellation was introduced, along with interesting things to see in each one. I particularly recall Cassiopeia, in which, between the two fainter stars Delta and Epsilon Cassiopeiae, lies the open cluster NGC 663. I first saw that cluster during the late summer of 1962. All Sidgwick had to say about it was that it can be spotted through binoculars. It didn't look like much, but I did spot it and then promptly forgot about it for more than sixty years. The other night, while conducting my search for comets, I encountered this star cluster again. This time it was one of the loveliest things I have ever seen. It moved me to tears.

I have since learned that NGC 663 is a grouping of about four hundred mostly big, bright, bluish suns. On a really dark night it might even be visible with the naked eye. An unusual feature is that the cluster happens to be positioned directly in front of a molecular cloud, which somehow blocks the background stars and allows the cluster to be even more beautiful. In a field of view already rich with stars in the Milky Way, the cluster stands out like a heavenly flower filled with diamonds.

NGC 663

I do have more to say about Sidgwick. In my youth I considered him a famous astronomer, but he is known mostly for the few books he wrote, especially *Introducing Astronomy*. Sidgwick enjoyed wide interests. He loved to hitchhike across the United States and Canada, and he edited a book of the shorter poems of Walter Savage Landor's shorter poems. Landor, Sidgwick's subject, had an unusual life, getting expelled both from Rugby School and from Oxford, where he allegedly shot a gun in his dormitory room. Reading about him led me to his delightful poem "The Evening Star:"

Thy star O Venus! often changes
Its radiant seat above,
The chilling pole-star never ranges —
'Tis thus with Hate and Love.

And 'tis thus I return to NGC 663, a cluster of stars that warms my heart. Where have I been for the last sixty years, religiously watching the sky, searching successfully for comets, enjoying many far-off stars and galaxies, but largely ignoring one of Nature's most wondrous splendors?

What Is a Philosopher Doing in Planetary Defense?

By Joel Marks, Professor Emeritus of Philosophy, University of New Haven (jmarks@newhaven.edu, www.docsoc.com)
2023 July 4



I am a philosopher. What does that mean? It could mean simply that I have a Ph.D. in philosophy (so I am a doctor of philosophy of philosophy!) and have had a career as a professional philosopher with the title “professor”: teaching philosophy courses, publishing in philosophy journals, speaking in colloquia and symposia, writing monographs, and so on. But Socrates himself would have looked down on such doings as the work of a sophist, not a philosopher, since philosophizing for money has nothing to do with seeking wisdom. To be a philosopher is to be a certain kind of person, who from love or sheer drive strives to understand everything, and in the process of seeking truth cultivates a critical skepticism toward all claims to know what is true. Doing this can make the philosopher unpopular, since people are attached to their beliefs and values; so Socrates was, as he put it, a gadfly, and indeed, was finally put to death for his questionings of cherished assumptions. I must say, however, that I have been given the most cordial welcome and attention by the scientists, engineers, and administrators I have come to know in planetary defense, even when we disagree.

There are also certain subject matters that most engage the philosopher’s soul, and in this I agree wholeheartedly with Immanuel Kant that “Two things fill the mind with ever new and increasing admiration and awe, the oftener and more steadily we reflect on them: the starry heavens above me and the moral law within me” (from the “Conclusion” of his *Critique of Practical Reason* (1788), Lewis White Beck translation). Thus it was that astronomy and ethics have been my own constant preoccupations, and so it is not a mystery why I would have become involved in an endeavor to bring planetary defense more in line with human values.

But I am neither a scientist nor a moralist. Again, I am a philosopher. So what is it that makes my dual preoccupation a valid mode of inquiry into things astronomical and ethical? The answer has to be: *method*. The philosopher, as I noted, looks critically at things, and does so in a very particular way, namely, by focusing on arguments. Here “argument” denotes not people bickering but rather giving reasons for claims and logically assessing the inferences from the reasons to the claims. It is a curious fact that the philosopher is less concerned about facts and more about the relations between facts. Insofar as the philosopher does adduce facts, they usually come in the form of things already known (and in this, I would argue, lies the main distinction from the scientist, who discovers or generates new facts or knowledge in support of claims or hypotheses). As Ludwig Wittgenstein put it: “The work of the philosopher consists in assembling reminders for a particular purpose” (item #127 from his *Philosophical Investigations* (1958, 2nd ed.), G.E.M. Anscombe translation).

Let me now illustrate all of the above with reference to planetary defense. My particular concern is the current focus on protecting us from impacts by smallish asteroids, which could obliterate a city or even a region (for example, the Eastern Seaboard or Europe). I contend that larger objects – whether asteroid or comet -- comparable to the impactor that presumably caused the mass extinction of 66 million years ago (most famous for wiping out the nonavian dinosaurs) merit equal or even greater attention. There are two sorts of reasons why the larger objects are relatively ignored today. One is that they would be much more difficult to defend against. The other is that they constitute a much smaller portion of the near-Earth objects. All in all, then, it is felt that our finite resources should be devoted to the more likely and tractable threat.

What Is a Philosopher Doing in Planetary Defense?

As plausible as that reasoning may sound, I consider it unsound. As a philosopher, I won't contest the facts, which I credit the scientists with having revealed to us. However, as I shall argue, the claim that the smaller objects merit more attention than the larger objects is not logically supported by those facts; in philo-speak, the conclusion does not follow from the premises and in fact relies on a number of fallacies of reasoning. I will consider them one by one.

The argument from ignorance

A prominent administrator at NASA was quoted in a news article as saying, "We know everything out there that is that big, and there is just nothing right now that's in an orbit that's any threat toward the Earth." I won't bother to name names since it is always possible the reporter or the editor got it wrong, or the administrator was speaking in an offhand or rushed manner; but I cite the remark because I have read and heard things like that over and over and, intentionally or not, they are highly misleading. The statement, or double statement, as written is simply false: We *don't* know everything out there that is that big (meaning, the size of a dinosaur-killer), and hence we *don't* know if one of them is a threat to us. The general fallacy at play here is that the extent of our present knowledge exhausts what there is to know. But of course it does not. Indeed, we could even phrase it ironically to say that we *know* it does not, and *never* could in the case of large potential impactors, because, for example, *at any moment* a large comet never before seen could be detected hurtling toward imminent collision with Earth from a reservoir containing *trillions* of comets in our Oort Cloud as well as the Oort Clouds of other solar systems in the galaxy. "If we don't know about it, it isn't there" is not a wise basis for policy.

The argument from regularity

Another fallacy commonly encountered in planetary defense is that probability implies regularity. Consider this remark (reported by RT News) by the Russian Emergency Minister Vladimir Puchkov concerning the lack of preparedness for the meteor explosion that took place over Chelyabinsk in 2013: "We thought that humanity would not have to face such an attack for another couple of thousand years, but the opposite happened and Russia was hit with a large-scale natural emergency." This is absurd. He seems to be saying that if we knew that the probability of an impact of this size was, say, 0.0003 or one in three thousand years, and the last one took place one thousand years ago, then the next one won't occur for another two thousand years. But that is not how it works. The probability in this kind of case represents an *average* of previously observed or inferred impacts; but this does not even rule out that there might be two such impacts in a single year, provided that this is "balanced" by no impactor for the following six thousands years. (And even this assumes that the pattern of past impacts will be maintained into the future.) Thus regarding the dinosaur-killer of 66 million years ago, it has been calculated that the chance of such an impactor arriving in the inner solar system on a trajectory toward Earth in any given year is one in 100 million. Therefore we have all the time in the world until the next one? Nonsense. It could show up today.

What Is a Philosopher Doing in Planetary Defense?

The argument from probability

Along similar lines to the argument from regularity is that the (presumed) fact that an impactor arrives in the inner solar system on a trajectory toward Earth only once every 100 million years means that we need not lose any sleep over, or take any urgent or dramatic steps to prevent, our possible extinction by impactor because, as I hear over and over, “it is highly unlikely.” Here as a philosopher I accept the scientifically determined fact, but still find the argument to be fallacious. The problem here is that the notion of probability has two quite distinct applications in this context. Suppose, for example, that the next dinosaur-killer impactor were about to wipe us out, and we knew it. We would then say that the chance of this object hitting the Earth this year (indeed, maybe *today*) is 1.0 or 100%. However, *even then* it might *still* be the case that the *average frequency* of *such* an event is only one in 100 million years. It does not matter that the last time there was such an impact was only 66 million years ago, nor that the present one will happen today. So again I say there is cold comfort in the *statistical fact*, and the conclusion that we need not take the threat of mass extinction seriously in our current planetary defense efforts cannot be drawn from that fact alone by a valid inference. Our extinction by impactor would be “highly unlikely” *whenever* it occurred. On the other hand (but by the same token), our extinction by impactor is *guaranteed* – a 100% certainty – if we allow ourselves to be lulled indefinitely from taking adequate steps to prevent it by the mantra, “It’s highly unlikely.”

The argument from necessity

Another frequently recited mantra of planetary defense is “Find ‘em early.” Indeed, Donald K. Yeomans is famous for asserting that planetary defense has *three* imperatives: “[F]ind them early, find them early, and ... find them early” (p.139 of his book *Near-Earth Objects: Finding Them Before They Find Us* [Princeton University Press, 2013]). Certainly no one would dispute that there can be no planetary defense unless we detect a potential impactor before it impacts ... and the earlier the better to allow for all the steps required to prevent the impact. However, it is fallacious to infer from a necessary condition to a sufficient condition. So while it is indeed necessary for effective planetary defense to “find ‘em early,” it is hardly sufficient to do so. We must also have in place a means of deflecting or destroying the potential impactor to keep it from becoming an actual impactor. (The word “mitigation” is commonly used for this aspect of planetary defense, although strictly speaking “mitigation” means only to reduce the severity of something, whereas the objective here is to preclude the event entirely. It is also to be noted, however, that some aspects of planetary defense as it is now commonly conceived do include genuine mitigation, such as warning a population to relocate before an unpreventable or even just a possible impact.) Yeomans himself (in the same book) gives reason to believe that waiting to prepare for a possible impact until we detect a potential impactor is a suicidal strategy, since, for example, the typical comet apparition occurs at the distance of Jupiter’s orbit, since that is when the icy body will be activated and lit up by the Sun, but at that distance, and due to the tremendous speed of a body coming from the Oort Cloud due to Kepler’s Second Law, there might be only nine months until Earth intersection, and that would be vastly insufficient time to mount a reliable mitigation mission from scratch.

What Is a Philosopher Doing in Planetary Defense?

The argument from risk reduction

As more and more near-Earth objects are discovered, we are told that the risk of catastrophe by an impactor has been “reduced.” This is true, statistically speaking. But it is *false* in *two* respects that have direct bearing on planetary defense. First, as noted above, even “reducing” the “risk” of an extinction-level impact to an exceedingly low value, such as once every 100 million years, in no way *predicts* when the next dinosaur-killer impactor heading our way will show up at our cosmic doorstep. It could happen today. Second, I put “risk” in *scare* quote above because the word was being used there *inappropriately*. “Risk” is often used as synonymous with probability. But the technically proper use of “risk” encompasses not only probability but also the value of the consequence whose probability has been calculated. And in the case of an extinction-size impactor, the value of the consequence is, arguably, infinite. That is because (and here is the ethicist in me speaking) *everything* that human beings value is a subjective function of human desires, and hence if all human beings ceased to exist forever, *every* valued thing would go out of existence forever too. Actually, however, that may itself be a fallacious argument; but without going into the philosophical minutiae of why I for one think it is, I do nevertheless maintain that, aside from folks such as the so-called anti-natalists who argue that human existence is net awful, just about everyone highly values things that would cease to exist if humanity, or even “just” human civilization, went out of existence – beginning with oneself and one’s children and one’s grandchildren and extending to the music of Beethoven and the Beatles and whatever institutions one would like to see continuing or improved “in perpetuity” and various projects one has put effort into or even devoted one’s life to and on and on and on. (I do not even consider the supposedly *objective* value of various things, such as human consciousness, or all sentient life, or all life.) So if this is not literally infinite in value, it could still very well amount to a sufficient magnitude to yield a huge negative value for its elimination ... and hence, even if “highly unlikely,” a very *high risk*. Therefore, I argue, the only way *this* risk can *truly* be *reduced* is to take the possibility of our extinction by a large impactor at short notice very seriously and, in practical terms, build a mitigation infrastructure sufficient to deflect or destroy a dinosaur-killer asteroid or comet heading our way *before* it is discovered and starting *today*.

Therefore I conclude that the possibility of an impact by a large object merits at least as much attention as that by a relatively small object, because the smaller probability of a large impact is more than offset by the negative value of its consequences, and even the small probability tells us nothing whatever about when the next such impact will occur if we don’t prevent it. So the job now is to rally support for dramatically increased funding for planetary defense and with a sense of urgency, akin to the Manhattan Project or the Apollo Program, by informing and lobbying the citizenry and policymakers. There will also need to be significant negotiations by international bodies, given the mix of law and politics that currently inhibits a comprehensive planetary defense. Then it will be up to the scientists and engineers to, in the words of Capt. Jean-Luc Picard, make it so.

Owens Valley Radio Observatory tour (photo essay)

by Ms. Michelle Evans, Author, Bestseller "*The X-15 Rocket Plane, Flying the First Wings into Space*"

Founder and President, Mach 25 Media (www.Mach25Media.com)

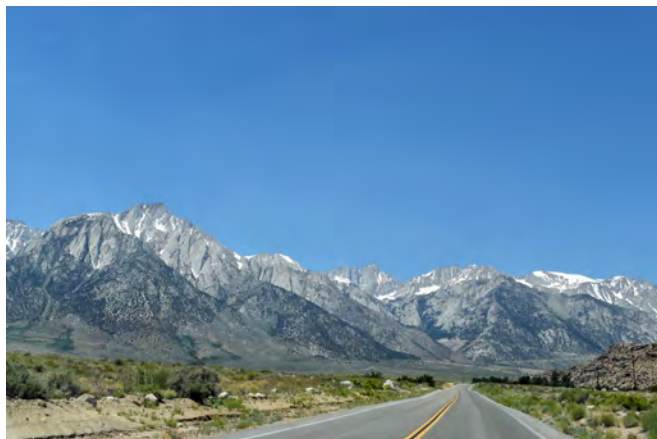
AIAA Distinguished Speaker, Writer, Photographer, and Communications Specialist in aerospace

Introduction

The Owens Valley Radio Observatory is located a few miles east of Big Pine, California. It is run by the Astronomy department of the California Institute of Technology (CalTech) in Pasadena, and is one of the largest such facilities in the world. Their mission, since the observatory's founding in 1956, is to glean scientific discoveries from the universe by listening to radio whispers from space. The facility's current director is Dr. Mark Hodges, and he hosted a special open house and tour of the facility for a small group of people on June 24th. Many children were present for the event, so the focus was on making science not only understandable, but also fun.

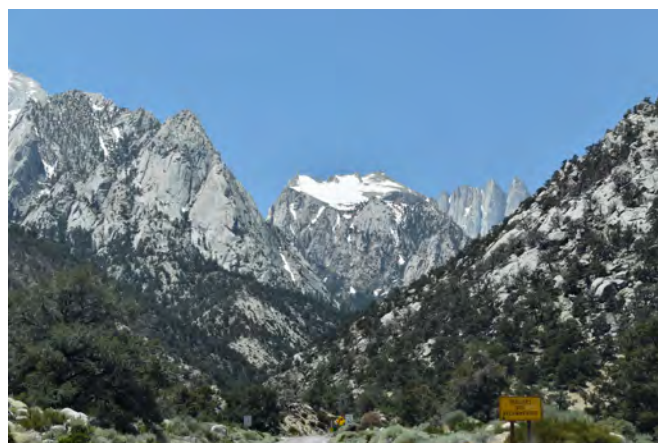
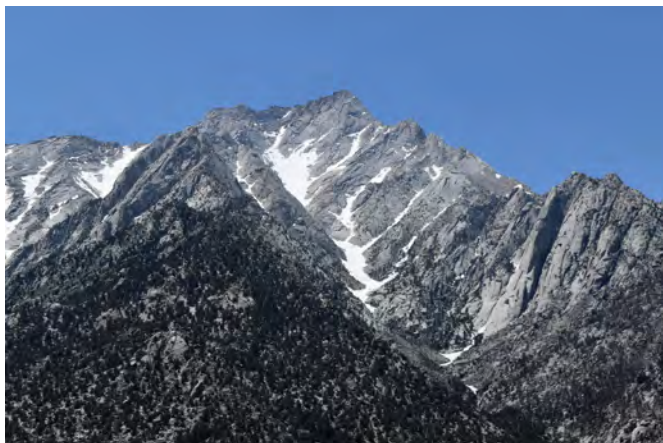
There are more than 100 radio telescopes currently at the Owens Valley site, including two 90-foot dishes and a 130-foot dish. Numerous smaller dishes carry out various programs, including the newly-established Deep Synoptic Array of 97 telescopes that will eventually be part of a network of 2000 such telescopes that will go online in the next few years in order to bring back some of the abilities that were lost when the 1000-foot radio telescope at Arecibo, Puerto Rico collapsed in December 2020.

Below is a photo essay of the events at the observatory on June 23rd and 24th. I want to thank Dr. Mark Hodges and Dr. Doug Millar of OVRO for their generous donation of their time to make this event possible.

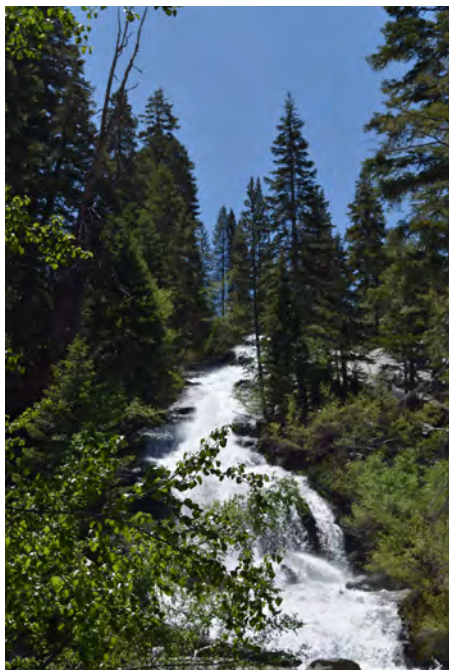


(Left) Approaching Mt. Whitney on US-395, heading north into the Owens Valley.

(Lower left and Lower right) Heading up the road to Whitney Portal.



Owens Valley Radio Observatory tour (photo essay)



(Left) A gushing waterfall at the top of Whitney Portal, 9300 feet up Mt. Whitney. If ever visiting OVRO, this is a must-see side trip, just 11 miles off US-395. (Right) Four miles east of Big Pine and US-395 is the entrance to the Owens Valley Radio Observatory grounds. Looking west, the Sun was nearing the horizon as I drove to the main buildings near the two 90-foot dishes.



(Upper left and upper right) Nearing the second 90-foot dish, the Sun disappears behind the support structure for the radio antenna.

(Left) The 90-foot dish lit up by the last rays of the Sun at 7:37 pm on June 23rd.



Owens Valley Radio Observatory tour (photo essay)



(Left) Looking down the row of telescopes set up for the Friday evening star party. The Owens Valley has some of the darkest skies in the United States. We were able to view numerous deep-sky objects, even before the crescent Moon set in the west. One of the highlights was being able to view the recently discovered supernova in the M101 galaxy. Knowing that the photons hitting my eyes through the telescope that evening had left the unnamed star 21 million years ago was a humbling experience.

(Right) A telephoto view of the largest telescope at OVRO, the 130-foot radio dish, more than a quarter of a mile east of the main complex. The second 90-foot radio dish is in the foreground between my viewpoint and the 130-foot scope, with another smaller dish close by.



(Left) Various sizes of waveguides used in the radio telescopes. (Bottom left / right) Creating homemade ice cream using liquid nitrogen as part of the science program.



Owens Valley Radio Observatory tour (photo essay)



(Left) The movie *Contact* featured a scientist from OVRO, and the star Jodie Foster sent a special signed t-shirt to the observatory as part of her thanks to the facility. It is now on display in the main building.

(Right) There is a planetary scale model that starts at the main building, then stretches all the way down to the 130-foot scope. Each foot equals 1 million miles, thus the "Earth" is 93 feet east of the "Sun." Here we are standing at the starting point of the planetary walk. The disc representing the Sun is between the men, and the end point is seen in the far distance. At this scale, the nearest star, Alpha Centauri, would be nearly all the way across the Atlantic Ocean in Europe!



(Upper Left) The two 90-foot dishes in the foreground, with the 130-foot dish in the distance. (Upper Right) Eclipse glasses were passed out to the guests so that they could safely view the Sun. There are two major solar eclipses coming up in the next months. On October 14th there will be an annular solar eclipse, and on April 8, 2024 there will be a total solar eclipse. Both of these eclipses will be visible from the United States, but only partial versions of these eclipses will be visible from California.

(Left) Cars and people in the foreground show the massive size of the 130-foot radio dish. (Right) A close-up of the backside of the dish, showing the gear mechanism and the catwalk at the base of the dish. We'll be taking a hike up inside the base to get to the catwalk shortly.



Owens Valley Radio Observatory tour (photo essay)



(Left and Right) We are now in the science program in the control room of the 130-foot telescope. Here Dr. Hodges shows one of the kids the effects of liquid nitrogen on a rose. First he freezes the rose, then has the kid clap his hands together, smashing the rose into tiny fragments



(Left) Soon after we finished in the control room, we headed for the climb up to the catwalk. I was first up the several stairwells that had to be climbed to get to the catwalk. At this point we were among the gears and pivots used to point the telescope to its various locations in the sky. The entire process is automated, so the dish would whirl and move while we were there.

(Right) The view westward, back toward the main buildings of OVRO, with several smaller dishes just below us. The landscape was magnificent from this vantage point.



(Left) Close up to one of the giant gears used to tilt the dish up and down.

(Right) The view from the catwalk, back down to where our cars were parked. The catwalk is approximately 100 feet above the floor of the valley.

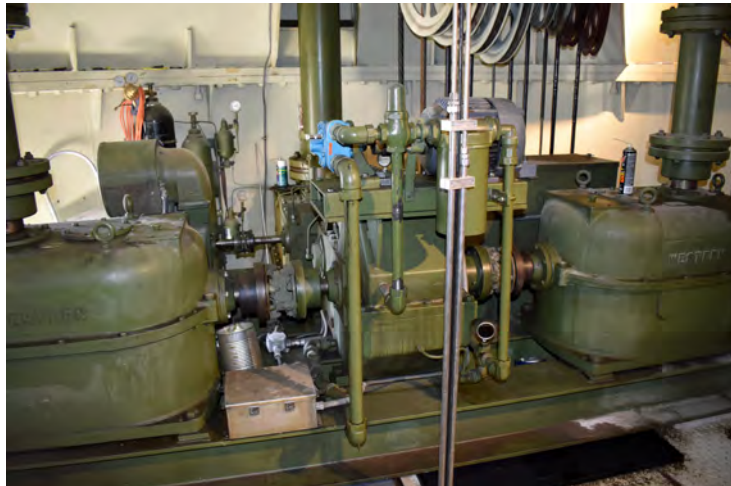


Owens Valley Radio Observatory tour (photo essay)



(Left) Looking back down the topmost set of stairs. This was the only stairway outside the base structure. The rest of the various staircases are inside.

(Right) The generators and motors inside the base that are used to move the giant dish above our heads.



(Upper Left) An inside stairway as I headed back down to the ground.



(Upper Right) Once again on terra firma, here is a look back up to where there are still a group of people up on the catwalk.



(Left) As several people exit the base, one person is still left at the top of the structure.

(Right) The view looking east, back toward the 130-foot antenna, as we were leaving the Owens Valley Radio Observatory.



Owens Valley Radio Observatory tour (photo essay)



In the distance is the 97 antenna Deep Synoptic Array. It was originally supposed to be 100 antennae, but several of the dishes were damaged and unusable, so just 97 dishes were left for the experiment. The idea is to gang together this large number of telescopes in order to simulate a much larger scope to look at the sky with more precision. Once all the kinks are worked out, it is hoped to create an array of 2000 of these scopes at a location, possibly in Nevada, to make up for the loss of the 1000-foot Arecibo dish.

(Right) A crescent Moon that I took on June 23rd at 7:11 pm. This was taken in the Owens Valley near the town of Big Pine

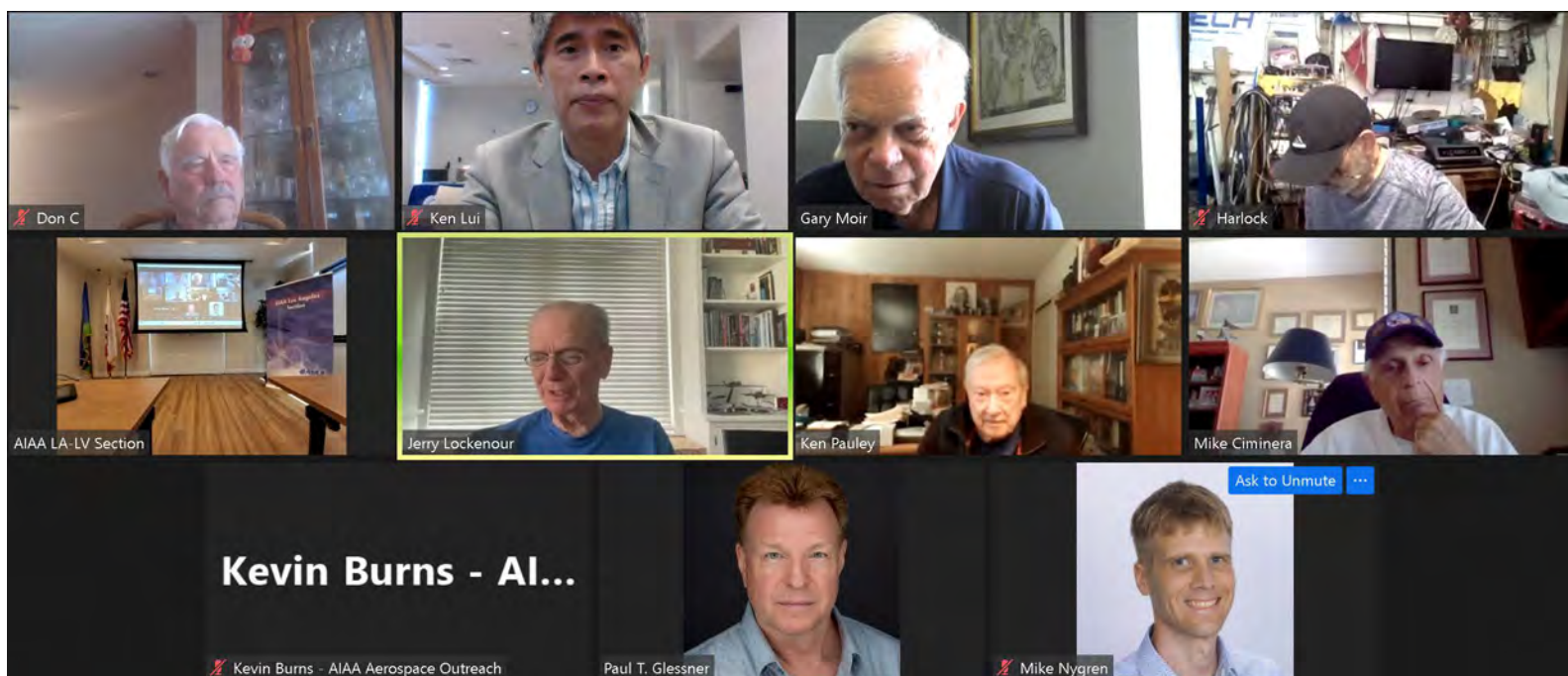


(2023 July 12) AIAA LA-LV Aero Alumni Meeting in June

(screenshots only) (<https://www.aiaa-lalv.org/blogs/2023-blogs/2023-july/2023-july-12>)



(Left) With a dedicated meeting room for the hybrid meeting, aero alumni (retirees from aerospace industries) could enjoy a better experiences for the hybrid meeting. (Right) A coffee machine was brought there, so in-person attendees could relax and enjoy if they wish.



Retirees from aerospace industries gathered again and discussed on various subjects, from the new book by Mr. Mike Ciminera, AIAA Domain initiatives, to aircraft designs, to the AIAA LA Section histories. It was fun and delightful for a conversation like this each month.

Falcon 9 Launch on July 19 (photo gallery)

by Ms. Michelle Evans, Author, Bestseller "*The X-15 Rocket Plane, Flying the First Wings into Space*"

Founder and President, Mach 25 Media (www.Mach25Media.com)

AIAA Distinguished Speaker, Writer, Photographer, and Communications Specialist in aerospace



Falcon 9 launch from Vandenberg SFB on the Central California coast at 9:09 pm PDT on July 19th. The photo was taken in Lake Forest approximately one minute after launch, with the SpaceX rocket going past the young crescent Moon.

Falcon 9 Launch on July 19 (photo gallery)



Falcon 9 Launch on July 19 (photo gallery)



Targeting Interplanetary Departures & Arrivals From The Moon

Danaiel R. Adamo, AIAA Associate Fellow, AIAA Distinguished Speaker (adamod@earthlink.net)

1.0 Introduction

Infrastructure in the Moon's vicinity serving as a human space flight (HSF) waypoint is being planned under NASA's Artemis Program. Dubbed *Gateway*, this infrastructure "is a destination for astronaut expeditions and science investigations, as well as a port for deep space transportation such as landers en route to the lunar surface or spacecraft embarking to destinations beyond the Moon."¹ Interplanetary HSF departures and arrivals at infrastructure orbiting the Moon entail an intermediate *Oberth effect* powered flyby of the Earth to minimize propellant consumption.² This flyby is all the more necessary in a HSF context because high thrust is used to minimize transit time and radiation/microgravity exposure to the crew.

Consequently, infrastructure in lunar orbit serving as an interplanetary transport terminal imposes additional geometric trajectory constraints versus direct departures to and arrivals from interplanetary space. Consider a conic (unperturbed) heliocentric trajectory Lambert problem³ solution connecting Earth with an interplanetary destination. When expressed as a patched conic Earth-centered trajectory, this solution accurately approximates a departure hyperbola *after* powered Earth flyby or an arrival hyperbola *before* powered Earth flyby.

This paper first seeks to document a parameter obtainable from any heliocentric Lambert solution and indicating lunar accessibility at the time of Earth arrival/departure. In an ordered array of Lambert solutions such as a porkchop chart (PCC),⁴ this parameter would reveal trends identifying optimal Earth departure/arrival dates supporting transfer from or to lunar orbit. Also documented are lunar transfer targeting techniques and relevant numeric results in the context of a notional HSF roundtrip mission to near-Earth object (NEO) 1999 AO₁₀.

Any heliocentric Lambert solution's Earth departure/arrival is associated with two geometric constraints relevant to lunar transfers.

- 1) $\mathbf{v}_\infty \equiv$ geocentric inertial asymptotic velocity on the hyperbolic departure or arrival trajectory.
- 2) $\beta \equiv$ the geocentric angle from $-\mathbf{v}_\infty$ (on departure) or $+\mathbf{v}_\infty$ (on arrival) to the hyperbolic trajectory's vertex, where the powered Earth flyby presumably occurs at perigee. This constraint is called the *asymptote angle* and it subtends the radius of a geocentric small circle called the locus of possible injection points (LPIP). The powered Earth flyby impulse is ideally one of the points on this locus.

To minimize arrival/departure-specific computations arising from the definition of β , the geocentric vector \mathbf{c} is defined as $-\mathbf{v}_\infty$ for Earth departures and as $+\mathbf{v}_\infty$ for Earth arrivals.

Starting with the heliocentric Lambert solution, \mathbf{v}_∞ is readily determined from the Earth departure/arrival velocity by subtracting Earth's heliocentric velocity at that time. This

¹ Reference <https://www.nasa.gov/content/about-gateway-deep-space-logistics> (accessed 16 July 2023).

² Reference the "Oberth effect" at https://en.wikipedia.org/wiki/Orbital_maneuver (accessed 16 July 2023).

³ Reference https://en.wikipedia.org/wiki/Lambert%27s_problem# (accessed 16 July 2023).

⁴ Reference https://en.wikipedia.org/wiki/Porkchop_plot (accessed 16 July 2023).

Targeting Interplanetary Departures & Arrivals From The Moon

computation is at the heart of patched conic theory.⁵ With the geocentric hyperbola's perigee distance r_P specified, β can be computed from Equation 1.

$$\beta = \operatorname{atan} \left\{ \frac{r_P c^2}{\mu_E} \sqrt{\frac{2\mu_E}{r_P c^2} + 1} \right\}, \mu_E \equiv \text{Earth's reduced mass} = 398600.435436 \text{ km}^3/\text{s}^2 \quad (1)$$

As illustrated by Figure 1, an ideal departure from lunar orbit would entail an elliptic geocentric transfer angle θ near 180° from the Moon's position r_M along the **blue** arc to the flyby perigee at r_P , first intercepting c and finally traversing the angle β . At r_P , a prograde Oberth impulse initiates hyperbolic Earth departure along $+v_\infty$.

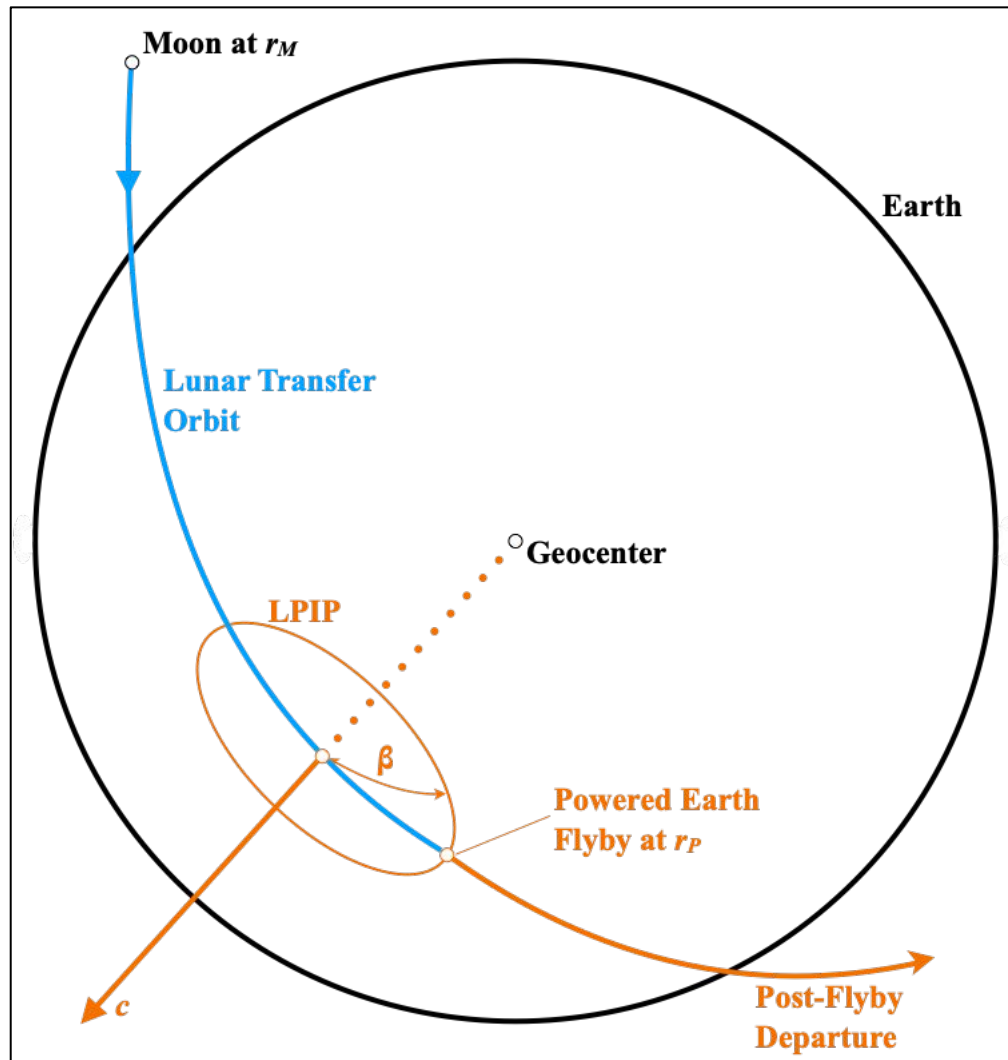


Figure 1 (not to scale). An ideal departure from the Moon's vicinity targeting an interplanetary destination entails an intermediary powered Earth flyby on the LPIP after intercepting c . The geocentric transfer angle θ is subtended by the **blue** arc.

⁵ Reference https://en.wikipedia.org/wiki/Patched_conic_approximation (accessed 2 July 2023).

Targeting Interplanetary Departures & Arrivals From The Moon

The Figure 1 departure sequence is reversed in an ideal arrival. Upon hyperbolic Earth return from interplanetary space, a retrograde impulse at r_P initiates an elliptic geocentric transfer angle θ near 180° to the Moon in which c is intercepted after an initial angle β is traversed. If $r_M = 384,400$ km (the Moon's mean geocentric distance) and $r_P = 6778.1$ km (400.0 km above Earth's equatorial radius), Kepler's third law provides the 180° transfer time Δt_X in Equation 2.

$$\Delta t_X = \pi \sqrt{\frac{\{0.5(r_M + r_P)\}^3}{\mu_E}} = 430425 \text{ s} = 4.98177 \text{ days} \quad (2)$$

This paper will assume $\Delta t_X = 5$ days for preliminary targeting, but deviations of ± 2 days from this value are certainly plausible in specific instances.

Mission trajectory segments described throughout this paper are defined by initial or terminal impulsive translational maneuvers. These events are described in Table 1. Similar event sequences could be applied to interplanetary destinations other than NEOs.

Table 1. Impulsive maneuver nomenclature associated with a NEO roundtrip mission is defined here for use in subsequent sections. Impulses are listed in chronologic order.

Impulse	Description
TEI	Trans-Earth Injection: this maneuver departs <i>Gateway</i> 's lunar orbit, initiates a near-Hohmann transfer to a powered Earth flyby, and targets Earth departure c -intercept.
TNI	Trans-NEO Injection: this maneuver is a prograde powered Earth flyby performed near a perigee height of +400 km and targets NEO intercept.
NAI	NEO Arrival Impulse: this maneuver is performed proximal to the NEO destination and halts NEO-relative motion.
NDI	NEO Departure Impulse: this maneuver is performed proximal to the NEO destination and targets Earth return c -intercept.
TLI	Trans-Lunar Injection: this maneuver is a retrograde powered Earth flyby performed near a perigee height of +400 km and initiates a near-Hohmann transfer targeting <i>Gateway</i> lunar orbit intercept.
LOI	Lunar Orbit Insertion: this maneuver enters <i>Gateway</i> 's lunar orbit.

2.0 Lunar Transfer Geometric Constraints

Given an Earth departure date of t_D to interplanetary space at TNI, the Moon's geocentric position and velocity (r_M , v_M) are obtained at $t_D - \Delta t_X$. With an Earth arrival date t_A from interplanetary space at TLI, (r_M , v_M) are obtained at $t_A + \Delta t_X$.

Targeting Interplanetary Departures & Arrivals From The Moon

The Moon's specific angular momentum vector \mathbf{h} is then determined with Equation 3.⁶

$$\mathbf{h} = \mathbf{r}_M \times \mathbf{v}_M \quad (3)$$

To minimize propulsive steering costs during powered Earth flyby, the Δt_X transfer plane must contain \mathbf{c} . If the geocentric transfer angle θ is sufficiently close to 180° , transfer flight path angle γ at \mathbf{r}_P will closely match that of the hyperbolic departure/arrival trajectory's perigee, defined to be zero at this position. Thus, the " θ near 180° " condition also tends to minimize radial steering losses during powered Earth flyby. In the context of lunar transfers to and from a powered Earth flyby, θ is therefore the accessibility parameter being sought in applications such as porkchop processing.

Equation 4 is evaluated to obtain a preliminary value for θ named $\tilde{\theta}$.

$$\tilde{\theta} = \arccos \left\{ \frac{\mathbf{c} \cdot \mathbf{r}_M}{cr_M} \right\} + \beta \quad (4)$$

A preliminary value $\tilde{\omega}$ for the transfer's geocentric rotation vector ω is then computed.

$$\tilde{\omega} = \mathbf{r}_M \times \mathbf{c} \text{ (departures only)} \quad (5a)$$

$$\tilde{\omega} = \mathbf{c} \times \mathbf{r}_M \text{ (arrivals only)} \quad (5b)$$

The sign of $\mathbf{h} \cdot \tilde{\omega}$ determines the direction of the transfer and leads to prograde values of θ and ω according to the following logic.⁷

$$\text{If } \mathbf{h} \cdot \tilde{\omega} \geq 0, \theta = \tilde{\theta} \text{ and } \omega = \tilde{\omega} \quad (6a)$$

$$\text{If } \mathbf{h} \cdot \tilde{\omega} < 0, \theta = 360^\circ - \tilde{\theta} \text{ and } \omega = -\tilde{\omega} \quad (6b)$$

Determining ω uniquely defines the transfer plane and permits hyperbolic perigee position and velocity to be determined. First compute the inertial-to-UVW transformation in the transfer plane at \mathbf{c} using Equation 7.

$$M_I^{UVW} = \begin{bmatrix} [\text{unit}(\mathbf{c})]^T \equiv \mathbf{U}^T \\ [\omega \times \mathbf{c}]^T \equiv \mathbf{V}^T \\ [\text{unit}(\omega)]^T \equiv \mathbf{W}^T \end{bmatrix} \quad (7)$$

⁶ Depending on the units and computation platform in use, caution should be exercised when computing \mathbf{h} and parameters depending on it because large values can arise. For example, units of km and s will produce h magnitudes on the order of $10^6 \text{ km}^2/\text{s}$. When further multiplied by \mathbf{r}_M , numeric precision may degrade. In contexts where only the direction of \mathbf{r}_M is significant, its components can be scaled with factors like $1/400,000 \text{ km}^{-1}$ to avoid inaccuracies.

⁷ In this context, "prograde" is with respect to the Moon's geocentric orbit plane; not Earth's equator. These two planes will be inclined to each other from 18.5° to 28.5° at a particular time. Thus, a marginally prograde transfer trajectory between \mathbf{r}_M and \mathbf{c} may exhibit retrograde westerly motion with respect to Earth's equator.

Targeting Interplanetary Departures & Arrivals From The Moon

At this point, it is important to recall ideal departures pass through c *before* reaching r_P while traversing the geocentric angle β . A departure r_P therefore has a positive V component. In contrast, ideal arrivals pass through c *after* reaching r_P while traversing the geocentric angle β . An arrival r_P therefore has a negative V component. Inertial geocentric position at the powered Earth flyby is then given as follows.

$$\mathbf{r}_P = [M_I^{UVW}]^T \begin{bmatrix} r_P \cos \beta \\ r_P \sin \beta \\ 0 \end{bmatrix} \text{ (departures only)} \quad (8a)$$

$$\mathbf{r}_P = [M_I^{UVW}]^T \begin{bmatrix} r_P \cos \beta \\ -r_P \sin \beta \\ 0 \end{bmatrix} \text{ (arrivals only)} \quad (8b)$$

Since r_P is defined to be at perigee for the hyperbolic arrival/departure trajectory, the unit vector of hyperbolic perigee velocity can be computed as well.

$$\mathbf{V}_P = \text{unit}(\mathbf{W} \times \mathbf{r}_P) \quad (9)$$

If hyperbolic perigee velocity v_P is required, \mathbf{V}_P can be scaled with the energy integral as follows.

$$v_P = \sqrt{\frac{2\mu_E}{r_P} + c^2 \mathbf{V}_P} \quad (10)$$

Because θ is generally not precisely 180° , computing velocities in the lunar transfer ellipse is left to solution of the geocentric Lambert problem with \mathbf{r}_M , \mathbf{r}_P , and Δt_X boundary values (where Δt_X may be refined through iteration to values other than 5 days).

From parameters already developed in this section, a hyperbolic conic geocentric inertial state vector $[\mathbf{r}, \mathbf{v}]^T$ can be computed for any specified true anomaly ϕ .⁸ Start by computing the hyperbola's eccentricity e and semi-latus rectum p .

$$e = \frac{1}{\cos \beta} \quad (11)$$

$$p = \frac{r_P^2 v_P^2}{\mu_E} \quad (12)$$

The inertial-to-perifocal transformation M_I^{PQW} is then computed.

$$M_I^{PQW} = \begin{bmatrix} [\text{unit}(\mathbf{r}_P)]^T \equiv \mathbf{P}^T \\ [\mathbf{W} \times \mathbf{P}]^T \equiv \mathbf{Q}^T \\ [\text{unit}(\boldsymbol{\omega})]^T \equiv \mathbf{W}^T \end{bmatrix} \quad (13)$$

⁸ Reference Bate, Mueller, and White, *Fundamentals of Astrodynamics*, Dover Publications, Inc., (1971), pp. 72-73.

Targeting Interplanetary Departures & Arrivals From The Moon

Note all perifocal positions and velocities on the conic hyperbolic trajectory lie in its plane and have zero W component. Inertial position and velocity then follow for any ϕ .

$$r = \frac{p}{1 + e \cos \phi} \quad (14)$$

$$\mathbf{r} = r [M_I^{PQW}]^T \begin{bmatrix} \cos \phi \\ \sin \phi \\ 0 \end{bmatrix} \quad (15)$$

$$\mathbf{v} = \sqrt{\frac{\mu_E}{p}} [M_I^{PQW}]^T \begin{bmatrix} -\sin \phi \\ e + \cos \phi \\ 0 \end{bmatrix} \quad (16)$$

3.0 Geocentric Lambert Lunar Transfer Targeting

Transfer trajectories between the Moon's center and a powered Earth flyby hyperbolic vertex are appropriate for overviews like PCCs tabulating associated θ values, but they suffer from two limitations. First, the transfer begins (for Earth departures) or ends (for Earth arrivals) at the inaccessible Moon's center \mathbf{r}_M , while a geocentric position in lunar orbit \mathbf{r}_O is programmatically more meaningful. When a geocentric transfer angle references \mathbf{r}_O as one of its legs, θ_O will convey that pedigree. Second, position and velocity along the transfer trajectory are unknown.

A geocentric Lambert solution for the transfer trajectory is therefore sought as an initial conic approximation ignoring Sun/Moon gravity and other perturbations. To enforce Figure 1 geometry, one of this solution's boundary conditions must be \mathbf{c} as specified in Table 2.

Table 2. Boundary conditions (BCs) for geocentric Lambert lunar transfer targeting depend on whether context is an interplanetary Earth departure or arrival.

Lambert BC	Earth Departure	Earth Arrival
Initial Position	\mathbf{r}_O at TEI	\mathbf{c} after TLI
Final Position	\mathbf{c} before TNI	\mathbf{r}_O at LOI

Although partial-revolution Lambert solutions will be nearly mandatory for crewed transfers, any number of complete geocentric revolutions can be considered if appropriate. Transfer time Δt_X will likely use an initial guess of 5 days for consistency with the θ selected from a PCC.

However, $\Delta t_X = 5$ days reflects an \mathbf{r}_M pedigree. In general, Δt_X will require iteration to shift the \mathbf{r}_O BC (and the transfer's semi-major axis) in inertial space such that true anomaly ϕ at \mathbf{c} -intercept is $-\beta$ (approaching perigee) for Earth departures or $+\beta$ (departing perigee) for Earth arrivals. These conditions preserve Figure 1 geometry for the transfer. The choice between Short-Way (Type I) and Long-Way (Type II) BCs will tend to favor prograde geocentric motion in the Lambert solution because the Moon's geocentric orbit is also prograde. Propellant required to depart or arrive at \mathbf{r}_O is thereby reduced.

Targeting Interplanetary Departures & Arrivals From The Moon

4.0 Precision Trajectory Targeting Considerations

Initial geocentric lunar transfer and heliocentric Earth departure/arrival Lambert solutions are each evolved into precision trajectories, thereby incorporating gravity and other perturbations to conic motion, through differential corrections (DCs) based on state transition matrices.⁹ Convergence is achieved when terminal position matches that being targeted to within 0.1 km. The DC process is relatively unstable when targeting terminal conditions deep in a gravity well. For an Earth departure scenario, this situation arises when targeting TNI's powered Earth flyby from the Moon's vicinity. In addition, DC iterations are unlikely to converge if a TLI powered Earth flyby is directly targeted from interplanetary initial conditions.

Powered Earth flyby DC targeting difficulties are managed by a staged approach. For example, a lunar transfer ending in TNI at r_P first targets a position about one hour beforehand, approximately 20,000 km from the geocenter. This precision lunar departure solution typically converges in less than five DC iterations when seeded with an initial lunar departure guess from the transfer's Lambert solution.¹⁰ This DC solution then seeds a rapidly convergent initial guess targeting r_P over the full Δt_X interval. When targeting r_P from interplanetary space, three or more DC runs may be required at progressively more proximal Earth distances, each solution seeding the next.

As a precision geocentric hyperbolic trajectory evolves from its Lambert baseline, care must be taken to update β and c , thus capturing changes to Figure 1 geometry from perturbations to conic motion. These changes will affect lunar transfer targeting as well. Suppose DC targeting has converged on a geocentric hyperbolic state vector $[\mathbf{r}, \mathbf{v}]^T$ near r_P . The following formulae provide a β update from this state.

$$a = \frac{1}{\frac{2}{r} - \frac{v^2}{\mu_E}} \quad (17)$$

$$v_\infty = \sqrt{\frac{-\mu_E}{a}} \quad (18)$$

$$\beta = \text{atan} \left\{ \frac{r_P v_\infty^2}{\mu_E} \sqrt{\frac{2\mu_E}{r_P v_\infty^2} + 1} \right\} \quad (19)$$

The inertial-to-perifocal transformation M_I^{PQW} , computed as follows, is essential to a c update.

$$\mathbf{h} = \mathbf{r} \times \mathbf{v} \quad (20)$$

⁹ This DC process is developed and applied throughout in D. R. Adamo, "Apollo 13 Trajectory Reconstruction via State Transition Matrices", *Journal of Guidance, Control, and Dynamics*, Vol. 31, No. 6, November-December 2008, pp. 1772-1781, DOI 10.2514/1.34977, <https://arc.aiaa.org/doi/10.2514/1.34977>.

¹⁰ In practice, it may be useful to generate a conic ephemeris with the Lambert solution's lunar departure state vector serving as initial conditions. The perigee minus one hour position and UTC to be targeted in the initial transfer DC run can readily be obtained from this ephemeris.

Targeting Interplanetary Departures & Arrivals From The Moon

$$\mathbf{e} = \frac{\mathbf{v} \times \mathbf{h}}{\mu_E} - \frac{\mathbf{r}}{r} \quad (21)$$

$$M_I^{PQW} = \begin{bmatrix} [\text{unit}(\mathbf{e})]^T \equiv \mathbf{P}^T \\ [\mathbf{W} \times \mathbf{P}]^T \equiv \mathbf{Q}^T \\ [\text{unit}(\mathbf{h})]^T \equiv \mathbf{W}^T \end{bmatrix} \quad (22)$$

Then \mathbf{c} is determined according to the following logic.

$$\mathbf{c} = v_\infty [M_I^{PQW}]^T \begin{bmatrix} \cos\beta \\ -\sin\beta \\ 0 \end{bmatrix} \quad (\text{departures only}) \quad (23a)$$

$$\mathbf{c} = v_\infty [M_I^{PQW}]^T \begin{bmatrix} \cos\beta \\ +\sin\beta \\ 0 \end{bmatrix} \quad (\text{arrivals only}) \quad (23b)$$

To obtain a state vector on the evolved hyperbolic conic trajectory at any specified true anomaly ϕ (reference Equations 14 through 16), it is only necessary to compute the evolved semi-latus rectum p .

$$p = r_p(1 + e) \quad (24)$$

5.0 Illustrative Targeting Examples

A roundtrip crewed mission to NEO 1999 AO₁₀, estimated to be from 29 m to 129 m in diameter, provides multiple Earth departure and return targeting examples from the 2025-26 timeframe.¹¹ In a bygone era from NASA's HSF planning circa 2010, NEOs like 1999 AO₁₀ served as incremental "steppingstone" destinations between the Moon and Mars.

The most accessible NEOs, those offering roundtrip mission durations less than six months and propulsive requirements less than a lunar landing, are in heliocentric orbits very similar to Earth's. Although an accessible NEO orbit typically has very small ecliptic inclination, proximity to Earth during a favorable mission opportunity can impose \mathbf{c} orientations with large latitudes on the ecliptic plane. Such orientations can produce challenged targeting geometries, particularly when departure or arrival at a position near the Moon and a powered Earth flyby must be integrated into mission design. A highly accessible NEO destination encourages selection of minimal v_∞ and β cases to reduce propulsive requirements. This can further challenge trajectory design because the associated LPIP is more localized in geocentric space.

¹¹ Reference

<https://cneos.jpl.nasa.gov/nhats/details.html#?des=1999%20AO10&dv=12&dur=450&stay=8&launch=2020-2045>
(accessed 27 June 2023).

Targeting Interplanetary Departures & Arrivals From The Moon

The trajectory predictor used in example DC runs is WeavEncke configured with 5-minute fixed numeric integration time steps.¹² Newtonian gravity acceleration from the Earth, Sun, and Moon is always simulated. When the WeavEncke conic reference body is Earth, a GEM 10 gravity harmonics model truncated beyond seventh degree and order is also invoked.¹³

Targeted translational maneuvers from Table 1 are simulated impulsively. Conditions immediately prior to an impulse are indicated with a minus "-" suffix, and those immediately following an impulse are appended with a plus "+" suffix.

The heliocentric JPL#17 ephemeris for 1999 AO₁₀ is accessed via JPL's *Horizons* server.¹⁴ Note the pedigree of this ephemeris is currently only 73 observations over 33 days, presumably when 1999 AO₁₀ was discovered early in 1999. The JPL#17 solution may therefore see substantial revision soon if 1999 AO₁₀ is recovered during its next close Earth approaches. Earth, Sun, and Moon ephemerides used are from JPL's DE441 configuration.¹⁵

5.1 Lunar Orbit Initial And Terminal Conditions

State vectors at which trajectories depart from and arrive in lunar orbit (at TEI- and LOI+, respectively) are defined at apocynthions of a notional nearly rectilinear halo orbit (NRHO).¹⁶ To render the NRHO state time-independent so it may be used in all departure/arrival cases, its selenocentric inertial Cartesian components are expressed in the Moon's equator and prime meridian (EPM) coordinate system at the pertinent epoch. In the right-handed convention, EPM is defined by the unit vector product $\mathbf{I}_M \times \mathbf{J}_M = \mathbf{K}_M$, where \mathbf{I}_M is directed at selenographic coordinates (zero latitude, zero longitude), \mathbf{J}_M is directed at selenographic coordinates (zero latitude, 90° E longitude), and \mathbf{K}_M is directed at selenographic latitude 90° N.

The NRHO apocynthion Cartesian EPM state appears in Table 3. It has a selenographic latitude = 78.849° N, longitude = 134.831° E, and altitude = +68,640.0 km. Selenocentric speed is 0.071597 km/s directed at an azimuth 132.063° west of selenocentric north in the local selenocentric horizontal plane. Osculating pericynthion height is +950.8 km, and osculating EPM inclination is 98.3°. Orbit stability of this NRHO evaluated at a particular time will depend on the evaluation interval in UTC and is beyond the scope of this paper.

Table 3. The following Moon-centered apocynthion state vector in a *Gateway*-like NRHO serves as time-independent initial conditions for lunar orbit departures (TEI-) and as terminal conditions for lunar orbit arrivals (LOI+).

EPM Position (km)	EPM Velocity (km/s)
$\begin{bmatrix} -9595.325 \\ +9652.213 \\ +69048.833 \end{bmatrix}$	$\begin{bmatrix} +0.004518 \\ +0.070850 \\ -0.009276 \end{bmatrix}$

¹² Reference D. R. Adamo, "A Precision Orbit Predictor Optimized for Complex Trajectory Operations," *Astrodynamics 2003, Advances in the Astronautical Sciences*, Vol. 116, Univelt, San Diego, CA, 2003, pp. 2567–2586.

¹³ Reference <https://agupubs.onlinelibrary.wiley.com/doi/abs/10.1029/JB084iB08p03897> (accessed 27 June 2023).

¹⁴ Reference <http://ssd.jpl.nasa.gov/?horizons> (accessed 27 June 2023).

¹⁵ Reference https://ssd.jpl.nasa.gov/doc/de440_de441.html (accessed 27 June 2023).

¹⁶ This NRHO has its apocynthion near the Moon's north pole, while current *Gateway* planning favors an NRHO with apocynthion near the lunar south pole to provide extended communications coverage thereto.

Targeting Interplanetary Departures & Arrivals From The Moon

5.2 Large-Scale Temporal Considerations For 1999 AO₁₀ Roundtrips In 2025-26

For the outbound heliocentric trajectory leg departing from Earth and arriving at 1999 AO₁₀, the most time-restrictive mission parameter appears to be NAI change-in-velocity magnitude Δv . The pertinent PCC appears in Figure 2. All PCC data appearing in this section are from Short-Way Lambert targeting to minimize flight time in the most favorable cases.

	A	B	C	D	E	F	G	H	I	J	K	L	M	N	O	P	Q	R	S	T
1	Earth Depart Date																			
2	1999 AO10	6/1/25	6/11/25	6/21/25	7/1/25	7/11/25	7/21/25	7/31/25	8/10/25	8/20/25	8/30/25	9/9/25	9/19/25	9/29/25	10/9/25	10/19/25	10/29/25	11/8/25	11/18/25	11/28/25
3	Arrive Date	10/8/04	11/4/01	12/03/8	12/731	13/491	14/349	15/364	16/639	18/396	21/156	26/395	40/598	199/785						
4	10/1/25	9/306	9/721	10/167	10/649	11/168	11/735	12/376	13/130	14/085	15/418	17/539	21/651	32/967	161/098					
5	10/11/25	8/047	8/287	8/570	8/885	9/223	9/586	9/984	10/431	10/962	11/646	12/620	14/227	17/436	26/481	130/571				
6	10/21/25	7/089	7/104	7/226	7/399	7/597	7/812	8/047	8/301	8/590	8/943	9/411	10/119	11/351	13/922	21/421	108/839			
7	11/10/25	6/725	6/233	6/133	6/163	6/245	6/350	6/470	6/601	6/746	6/920	7/143	7/472	8/015	9/028	11/259	17/886	95/358		
8	11/20/25	9/043	8/997	8/345	8/167	8/132	8/148	8/189	8/240	8/301	8/378	8/480	8/638	8/904	9/389	7/350	9/483	15/758	87/897	
9	11/30/25	54/184	8/829	8/185	4/453	4/239	4/169	4/152	4/155	4/171	4/200	4/248	4/334	4/490	4/772	5/301	6/317	8/488	14/623	83/212
10	12/10/25	60/344	56/654	56/854	4/302	3/592	3/390	3/323	3/301	3/300	3/315	3/350	3/416	3/536	3/743	4/100	4/711	5/805	8/000	13/916
11	12/20/25	59/542	59/500	57/354	7/021	3/393	2/814	2/678	2/647	2/653	2/680	2/726	2/802	2/920	3/101	3/380	3/805	4/472	5/583	7/689
12	12/30/25	58/595	58/772	58/788	57/488	5/404	2/543	2/208	2/179	2/213	2/268	2/340	2/435	2/561	2/730	2/963	3/281	3/729	4/386	5/422
13	1/9/26	57/640	57/954	58/156	58/221	57/485	3/562	1/926	1/891	1/971	2/062	2/158	2/267	2/394	2/548	2/740	2/980	3/292	3/708	4/289
14	1/19/26	56/704	57/139	57/471	57/696	57/803	57/497	2/012	1/781	1/925	2/042	2/147	2/253	2/365	2/493	2/642	2/817	3/029	3/294	3/632
15	1/29/26	55/793	56/345	56/797	57/148	57/395	57/537	57/536	1/933	2/116	2/206	2/280	2/356	2/435	2/524	2/625	2/739	2/872	3/030	3/217
16	2/8/26	54/911	55/578	56/147	56/617	56/985	57/254	57/421	57/417	3/084	2/655	2/576	2/568	2/586	2/620	2/666	2/720	2/784	2/858	2/940
17	2/18/26	54/068	54/848	55/533	56/120	56/608	56/996	57/283	57/462	56/484	4/292	3/198	2/929	2/821	2/771	2/749	2/739	2/737	2/739	2/741
18	2/28/26	53/265	54/156	54/955	55/659	56/265	56/772	57/178	57/479	57/653	53/631	5/322	3/669	3/211	3/001	2/878	2/790	2/719	2/655	2/589
19	3/10/26	52/486	53/486	54/397	55/216	55/939	56/566	57/092	57/515	57/828	57/977	49/392	6/173	4/046	3/412	3/100	2/899	2/745	2/611	2/480
20	3/20/26	51/719	52/825	53/846	54/780	55/620	56/366	57/013	57/558	57/999	58/321	58/430	46/199	6/884	4/333	3/528	3/113	2/836	2/615	2/416
21	3/30/26	50/953	52/163	53/293	54/339	55/296	56/161	56/930	57/599	58/166	58/624	58/954	59/021	45/293	7/514	4/532	3/558	3/044	2/691	2/404
22	4/9/26	50/175	51/486	52/723	53/881	54/953	55/937	56/829	57/623	58/317	58/905	59/381	59/722	59/758	46/800	8/118	4/652	3/508	2/896	2/470
23	4/19/26	49/372	50/779	52/119	53/386	54/572	55/675	56/688	57/608	58/430	59/150	59/763	60/260	60/615	60/649	50/312	8/775	4/710	3/384	2/674
24	4/29/26	48/523	50/023	51/461	52/833	54/130	55/349	56/484	57/528	58/480	59/332	60/081	60/721	61/243	61/619	61/688	54/943	4/718	3/192	

Figure 2. Heliocentric Lambert solution values for NAI Δv in km/s are tabulated as a function of TNI date (columns) and NAI date (rows) at 10-day increments. Minimal values < 2.5 km/s are green in color. Boxed dates, together with Cell N13's $\Delta v = 2.394$ km/s, pertain to the preliminary outbound mission leg selection from TNI to NAI.

Selection of 29 September 2025 as the TNI date in Figure 2 is particularly tentative. The geocentric transfer angle θ between TEI and TNI is highly sensitive to the associated time interval as the Moon orbits Earth at 13.2° per day.

For 9 January 2026 NAI on Row 13, Figure 3's PCC also favors TNI dates in late September 2025 because TNI early that month is associated with an LPIP centered 40° or more *south* of Earth's equatorial plane (recall $c \equiv -v_\infty$ for TNI's Earth departure). The desired near-Hohmann transfer with θ close to 180° therefore requires the Moon be about 40° *north* of Earth's equator at TEI. Although the Moon can attain declinations up to 29° north of Earth's equator in September 2025, it only does so at ecliptic longitudes near 90° .¹⁷

Thus, c for the Cell L13 heliocentric Lambert solution must be near ecliptic longitude $90 + 180 = 270^\circ$ to accommodate a near-Hohmann geometric constraint, but the actual ecliptic longitude for c is near 324° . As a result, Figure 1's c -intercept geometry cannot be satisfied for early September 2025 TEI-to-TNI orbit transfers with TNI near perigee. Indeed, the Cell L13 geocentric transfer Lambert solution connecting TNI's c with the Moon five days earlier has a perigee 5000 km below Earth's surface with $\theta = 51.5^\circ$. Dramatic variations in θ during September 2025 illustrate differing time scales are in play between lunar and interplanetary transfer seasons for HSF planning. Whereas the latter tend to span weeks, the former are restricted to only a few days.

¹⁷ Ecliptic longitude is measured eastward on the geocentric celestial sphere from zero at the ecliptic's ascending node on Earth's equatorial plane, the first point of Aries. Consequently, near ecliptic longitude 90° , the Moon is as far north of Earth's equator as possible that month.

Targeting Interplanetary Departures & Arrivals From The Moon

	A	B	C	D	E	F	G	H	I	J	K	L	M	N	O	P	Q	R	S	T
1	Earth Depart Date																			
2	1999 AO10	6/1/25	6/11/25	6/21/25	7/1/25	7/11/25	7/21/25	7/31/25	8/10/25	8/20/25	8/30/25	9/9/25	9/19/25	9/29/25	10/9/25	10/19/25	10/29/25	11/8/25	11/18/25	11/28/25
3	Arrive Date	-2.242	-4.789	-6.734	-8.354	-9.383	-10.006	-10.330	-10.206	-9.909	-9.494	-9.046	-8.787	-8.685						
4	10/1/25	4.247	0.789	-1.793	-3.907	-5.218	-6.068	-6.572	-6.528	-6.348	-6.018	-5.610	-5.426	-5.339	-5.335					
5	10/11/25	15.387	10.330	6.630	3.680	1.925	0.720	-0.033	-0.058	-0.068	0.093	0.307	0.139	-0.067	-0.331	-0.528				
6	10/21/25	31.859	24.865	19.681	15.569	13.229	11.514	10.412	10.309	9.910	9.678	9.352	8.319	7.367	6.381	5.530	5.167			
7	11/10/25	49.654	42.316	36.501	31.673	29.036	26.908	25.475	25.239	23.980	22.818	21.219	18.544	16.279	14.065	12.159	11.012	10.487		
8	11/20/25	62.106	56.752	52.362	48.449	45.544	44.676	43.217	42.596	39.742	36.875	33.168	28.395	24.612	21.032	18.014	16.029	14.681	14.142	
9	11/30/25	32.426	64.185	62.574	60.986	60.810	59.959	58.701	57.054	52.046	47.189	41.409	35.103	30.294	25.771	21.995	19.413	17.402	16.245	15.855
10	12/10/25	10.824	21.769	65.546	67.297	69.405	70.005	68.754	65.345	58.299	51.972	45.028	38.131	32.957	28.039	23.927	21.053	18.625	17.061	16.287
11	12/20/25	7.594	6.311	13.693	66.738	72.368	75.254	73.988	68.611	60.119	52.975	45.557	38.580	33.404	28.413	24.215	21.265	18.611	16.815	15.827
12	12/30/25	5.786	3.439	1.785	6.830	68.883	76.576	76.611	69.516	59.797	52.020	44.340	37.397	32.354	27.415	23.245	20.345	17.593	15.683	14.614
13	1/9/26	4.369	1.726	-0.767	-2.735	0.456	72.135	78.243	69.671	58.176	49.559	41.609	34.717	29.872	25.113	21.049	18.316	15.572	13.643	12.617
14	1/19/26	3.109	0.349	-2.367	-4.971	-7.176	-5.925	77.389	68.938	53.814	44.047	36.076	29.503	25.158	20.847	17.052	14.680	12.110	10.272	9.455
15	1/29/26	1.925	-0.889	-3.682	-6.435	-9.066	-11.503	-12.828	56.446	35.161	27.577	22.571	18.010	15.303	12.389	9.319	7.759	5.756	4.185	3.890
16	2/8/26	0.780	-2.058	-4.873	-7.660	-10.361	-12.988	-15.654	-21.028	-43.508	-23.937	-13.078	-9.720	-7.526	-6.315	-7.598	-7.330	-7.712	-8.784	-7.760
17	2/18/26	-0.341	-3.187	-6.001	-8.780	-11.468	-14.073	-16.653	-19.513	-31.520	-61.831	-52.699	-47.625	-43.218	-38.712	-38.638	-35.953	-33.519	-33.378	-28.477
18	2/28/26	-1.448	-4.292	-7.090	-9.841	-12.486	-15.024	-17.479	-19.924	-22.975	-44.181	-67.683	-64.274	-61.449	-58.287	-56.994	-51.901	-47.515	-43.109	-35.358
19	3/10/26	-2.548	-5.381	-8.154	-10.864	-13.452	-15.908	-18.237	-20.443	-22.699	-25.885	-55.601	-70.798	-66.588	-62.568	-58.993	-51.861	-46.119	-40.038	-32.801
20	3/20/26	-3.643	-6.459	-9.199	-11.861	-14.381	-16.747	-18.952	-20.970	-22.863	-24.843	-28.046	-62.409	-71.131	-64.969	-59.137	-51.498	-44.782	-38.068	-31.097
21	3/30/26	-4.736	-7.529	-10.229	-12.834	-15.280	-17.548	-19.628	-21.479	-23.121	-24.618	-26.217	-29.268	-63.990	-69.887	-61.805	-53.221	-45.454	-38.022	-30.842
22	4/9/26	-5.825	-8.590	-11.245	-13.786	-16.149	-18.314	-20.265	-21.957	-23.389	-24.575	-25.586	-26.715	-29.382	-60.867	-67.772	-57.371	-48.228	-39.735	-31.906
23	4/19/26	-6.911	-9.642	-12.244	-14.715	-16.990	-19.044	-20.863	-22.395	-23.634	-24.573	-25.528	-26.694	-28.307	-54.034	-64.960	-53.518	-43.435	-34.427	
24	4/29/26	-7.992	-10.682	-13.225	-15.619	-17.797	-19.734	-21.414	-22.786	-23.838	-24.557	-24.938	-25.021	-24.892	-24.845	-26.070	-44.604	-62.499	-49.865	-38.937

Figure 3. Heliocentric Lambert solution values for δ_∞ , the TNI+ geocentric asymptotic velocity v_∞ declination on Earth's equator in degrees, are tabulated as a function of TNI date (columns) and NAI date (rows) at 10-day increments. Maximal values $> 57^\circ$ in magnitude are **red** in color. **Boxed** dates, together with Cell N13's $\delta_\infty = +29.872^\circ$, pertain to the preliminary outbound mission leg selection from TNI to NAI.

Turning next to the mission's return heliocentric trajectory leg from 1999 AO₁₀, Figure 4's NDI Δv PCC tends to be most constraining to the timeline. Particularly in the context of HSF, risks associated with a 1999 AO₁₀ roundtrip are difficult to justify if less than 10 days are spent at the destination, but delaying NDI any further results in appreciable Δv increases. The 19 January 2026 NDI date is therefore a good compromise between these conflicting influences.

	A	B	C	D	E	F	G	H	I	J	K	L	M	N	O	P	Q	R	S	T
1	Earth Depart Date																			
2	1999 AO10	10/31/25	11/10/25	11/20/25	11/30/25	12/10/25	12/20/25	12/30/25	1/9/26	1/19/26	1/29/26	2/8/26	2/18/26	2/28/26	3/10/26	3/20/26	3/30/26	4/9/26	4/19/26	4/29/26
3	Arrive Date	5.410	8.216	16.482	15.614															
4	11/30/25	3.939	5.263	7.859	15.614															
5	12/10/25	3.046	3.764	4.941	7.292	14.402														
6	12/20/25	2.401	2.808	3.413	4.426	6.485	12.770													
7	1/9/26	1.879	2.106	2.425	2.913	3.749	5.475	10.778												
8	1/19/26	1.420	1.538	1.698	1.931	2.302	2.956	4.324	8.541											
9	1/29/26	1.013	1.063	1.131	1.233	1.394	1.665	2.157	3.194	6.373										
10	2/8/26	0.682	0.689	0.707	0.744	0.815	0.942	1.164	1.565	2.390	4.853									
11	2/18/26	0.553	0.524	0.519	0.540	0.596	0.696	0.857	1.112	1.538	2.373	4.817								
12	2/28/26	0.769	0.699	0.680	0.701	0.759	0.857	1.004	1.217	1.538	2.065	3.102	6.178							
13	3/10/26	1.207	1.065	1.010	1.012	1.057	1.141	1.269	1.450	1.710	2.103	2.755	4.056	8.001						
14	3/20/26	1.813	1.523	1.396	1.356	1.372	1.431	1.532	1.678	1.885	2.186	2.643	3.411	4.984	9.808					
15	3/30/26	2.695	2.090	1.826	1.713	1.681	1.703	1.768	1.874	2.030	2.255	2.583	3.088	3.966	5.796	11.427				
16	4/9/26	4.280	2.866	2.333	2.094	1.989	1.959	1.980	2.042	2.147	2.305	2.536	2.880	3.435	4.430	6.514	12.919			
17	4/19/26	8.751	4.172	3.002	2.531	2.311	2.210	2.175	2.188	2.242	2.341	2.496	2.729	3.101	3.732	4.873	7.260	14.542		
18	4/29/26	49.311	7.405	4.077	3.092	2.672	2.464	2.360	2.317	2.318	2.362	2.453	2.605	2.862	3.302	4.055	5.413	8.220	16.671	
19	5/9/26	64.293	30.163	6.530	3.969	3.128	2.747	2.547	2.437	2.383	2.374	2.410	2.500	2.681	3.012	3.581	4.542	6.235	9.658	19.794
20	5/19/26	64.376	62.878	19.830	5.874	3.830	3.103	2.754	2.558	2.442	2.380	2.367	2.409	2.538	2.807	3.283	4.066	5.339	7.505	11.779
21	5/29/26	64.036	63.219	61.446	14.700	5.313	3.645	3.011	2.688	2.497	2.380	2.322	2.325	2.419	2.656	3.086	3.787	4.871	6.549	9.320
22	6/8/26	63.532	62.921	62.099	60.105	11.640	4.780	3.405	2.853	2.557	2.378	2.277	2.247	2.320	2.540	2.956	3.620	4.611	6.058	8.220
23	6/18/26	62.903	62.447	61.835	61.062	59.010	9.483	4.237	3.110	2.636	2.377	2.230	2.174	2.234	2.452	2.866	3.517	4.457	5.774	7.625
24	6/28/26	62.159	61.846	61.385	60.815	60.134	58.294	7.710	3.661	2.763	2.377	2.178	2.100	2.157	2.382	2.804	3.452	4.362	5.596	7.261

Figure 4. Heliocentric Lambert solution values for NDI Δv in km/s are tabulated as a function of NDI date (columns) and TLI date (rows) at 10-day increments. Minimal values < 2.5 km/s are **green** in color. **Boxed** dates, together with Cell J12's $\Delta v = 1.538$ km/s, pertain to the preliminary return mission leg selection from NDI to TLI.

Per Figure 4, moving TLI earlier by up to 10 days is certainly possible with little NDI Δv impact. However, TLI date selection must be considered preliminary pending θ PCC data with greater temporal resolution than 10 days.

Figure 5's PCC is dedicated to δ_∞ data on which LPIPs for TLI are centered. Pertinent Figure 5 values are much more nearly zero than those in Figure 3, indicating geometry governing return transfer from TLI to LOI will be more accommodating than that for lunar departure.

Targeting Interplanetary Departures & Arrivals From The Moon

	A	B	C	D	E	F	G	H	I	J	K	L	M	N	O	P	Q	R	S	T
1	1999 AO10 Depart Date																			
2	Earth Return	10/31/25	11/10/25	11/20/25	11/30/25	12/10/25	12/20/25	12/30/25	1/9/26	1/19/26	1/29/26	2/8/26	2/18/26	2/28/26	3/10/26	3/20/26	3/30/26	4/9/26	4/19/26	4/29/26
3	11/30/25	-8.266	-11.883	-14.448	-16.089	-17.721	-19.353	-20.985	-22.617	-24.249	-25.881	-27.513	-29.145	-30.777	-32.409	-34.041	-35.673	-37.305	-38.937	-40.569
4	12/10/25	-10.822	-13.607	-16.392	-19.177	-21.962	-24.747	-27.532	-30.317	-33.102	-35.887	-38.672	-41.457	-44.242	-47.027	-49.812	-52.597	-55.382	-58.167	-60.952
5	12/20/25	-13.383	-16.299	-19.215	-22.131	-25.047	-27.963	-30.879	-33.795	-36.711	-39.627	-42.543	-45.459	-48.375	-51.291	-54.207	-57.123	-60.039	-62.955	-65.871
6	12/30/25	-15.869	-19.929	-23.989	-28.049	-32.109	-36.169	-40.229	-44.289	-48.349	-52.409	-56.469	-60.529	-64.589	-68.649	-72.709	-76.769	-80.829	-84.889	-88.949
7	1/9/26	-17.931	-22.116	-26.201	-30.286	-34.371	-38.456	-42.541	-46.626	-50.711	-54.796	-58.881	-62.966	-67.051	-71.136	-75.221	-79.306	-83.391	-87.476	-91.561
8	1/19/26	-18.783	-23.088	-27.193	-31.298	-35.403	-39.508	-43.613	-47.718	-51.823	-55.928	-60.033	-64.138	-68.243	-72.348	-76.453	-80.558	-84.663	-88.768	-92.873
9	1/29/26	-19.556	-23.981	-28.106	-32.231	-36.356	-40.481	-44.606	-48.731	-52.856	-56.981	-61.106	-65.231	-69.356	-73.481	-77.606	-81.731	-85.856	-89.981	-94.106
10	2/8/26	-19.849	-24.394	-28.539	-32.684	-36.829	-40.974	-45.119	-49.264	-53.409	-57.554	-61.700	-65.845	-70.000	-74.145	-78.290	-82.435	-86.580	-90.725	-94.870
11	2/18/26	-19.895	-24.460	-28.615	-32.770	-36.925	-41.080	-45.235	-49.390	-53.545	-57.700	-61.855	-66.010	-70.165	-74.320	-78.475	-82.630	-86.785	-90.940	-95.095
12	2/28/26	-20.953	-25.538	-29.693	-33.848	-38.003	-42.158	-46.313	-50.468	-54.623	-58.778	-62.933	-67.088	-71.243	-75.398	-79.553	-83.708	-87.863	-92.018	-96.173
13	3/10/26	-22.373	-26.958	-31.113	-35.268	-39.423	-43.578	-47.733	-51.888	-56.043	-60.198	-64.353	-68.508	-72.663	-76.818	-80.973	-85.128	-89.283	-93.438	-97.593
14	3/20/26	-25.128	-29.713	-33.868	-38.023	-42.178	-46.333	-50.488	-54.643	-58.798	-62.953	-67.108	-71.263	-75.418	-79.573	-83.728	-87.883	-92.038	-96.193	-100.348
15	3/30/26	-30.318	-34.903	-39.058	-43.213	-47.368	-51.523	-55.678	-59.833	-63.988	-68.143	-72.298	-76.453	-80.608	-84.763	-88.918	-93.073	-97.228	-101.383	-105.538
16	4/9/26	-37.461	-42.046	-46.201	-50.356	-54.511	-58.666	-62.821	-66.976	-71.131	-75.286	-79.441	-83.596	-87.751	-91.906	-96.061	-100.216	-104.371	-108.526	-112.681
17	4/19/26	-46.042	-50.627	-54.782	-58.937	-63.092	-67.247	-71.402	-75.557	-79.712	-83.867	-88.022	-92.177	-96.332	-100.487	-104.642	-108.797	-112.952	-117.107	-121.262
18	4/29/26	-49.494	-54.079	-58.234	-62.389	-66.544	-70.699	-74.854	-79.009	-83.164	-87.319	-91.474	-95.629	-99.784	-103.939	-108.094	-112.249	-116.404	-120.559	-124.714
19	5/9/26	9.835	-40.130	-45.685	-50.840	-55.995	-61.150	-66.305	-71.460	-76.615	-81.770	-86.925	-92.080	-97.235	-102.390	-107.545	-112.700	-117.855	-123.010	-128.165
20	5/19/26	10.874	-49.511	-55.066	-60.221	-65.376	-70.531	-75.686	-80.841	-85.996	-91.151	-96.306	-101.461	-106.616	-111.771	-116.926	-122.081	-127.236	-132.391	-137.546
21	5/29/26	9.565	-6.978	-12.433	-17.888	-23.343	-28.798	-34.253	-39.708	-45.163	-50.618	-56.073	-61.528	-66.983	-72.438	-77.893	-83.348	-88.803	-94.258	-99.713
22	6/8/26	7.528	5.675	2.989	-5.451	-15.896	-26.341	-36.786	-47.231	-57.676	-68.121	-78.566	-89.011	-99.456	-109.901	-120.346	-130.791	-141.236	-151.681	-162.126
23	6/18/26	5.119	3.527	1.692	-0.961	-10.406	-20.851	-31.296	-41.741	-52.186	-62.631	-73.076	-83.521	-93.966	-104.411	-114.856	-125.301	-135.746	-146.191	-156.636
24	6/28/26	2.524	1.052	-0.488	-2.232	-4.711	-7.190	-9.669	-12.148	-14.627	-17.106	-19.585	-22.064	-24.543	-27.022	-29.501	-31.980	-34.459	-36.938	-39.417

Figure 5. Heliocentric Lambert solution values for δ_∞ consistent with TLI- are tabulated as a function of NDI date (columns) and TLI date (rows) at 10-day increments. Minimal values $< 28.5^\circ$ in magnitude are green in color. Boxed dates pertain to the preliminary return mission leg selection from NDI to TLI and also apply to Cell J12's $\delta_\infty = -7.632^\circ$.

5.3 Example Targeting TEI, TNI, And NAI Before 1999 AO₁₀ Loiter

Figure 6 is a PCC tabulating θ values at daily intervals as reckoned by outbound heliocentric Short-Way Lambert targeting from TNI to NAI. Color-coded θ intervals form vertical bands in this PCC because each column is 5 days after a potential TEI date and therefore corresponds to a specific lunar geocentric position r_M .

	A	B	C	D	E	F	G	H	I	J	K	L	M	N	O	P
1	Earth Depart Date															
2	1999 AO10 Arrive Date	9/18/25	9/19/25	9/20/25	9/21/25	9/22/25	9/23/25	9/24/25	9/25/25	9/26/25	9/27/25	9/28/25	9/29/25	9/30/25	10/1/25	10/2/25
3	1/2/26	255.0	243.0	231.3	220.0	209.6	200.4	193.7	168.9	166.4	160.2	151.9	142.7	133.0	123.1	113.1
4	1/3/26	255.0	242.9	231.2	219.9	209.4	200.2	193.5	169.0	166.4	160.0	151.7	142.4	132.7	122.7	112.7
5	1/4/26	255.0	242.9	231.1	219.8	209.2	200.0	193.2	169.2	166.4	159.9	151.5	142.1	132.3	122.3	112.3
6	1/5/26	255.0	242.9	231.0	219.7	209.0	199.7	193.0	169.4	166.5	159.8	151.3	141.8	132.0	121.9	111.8
7	1/6/26	255.0	242.8	231.0	219.5	208.9	199.5	192.7	169.6	166.5	159.7	151.1	141.5	131.6	121.6	111.4
8	1/7/26	255.0	242.8	230.9	219.4	208.7	199.3	192.5	169.8	166.6	159.6	150.9	141.3	131.3	121.2	111.0
9	1/8/26	255.0	242.8	230.8	219.3	208.5	199.1	192.2	170.0	166.7	159.6	150.7	141.0	131.0	120.8	110.6
10	1/9/26	255.1	242.8	230.8	219.2	208.4	198.9	191.9	170.2	166.8	159.5	150.5	140.7	130.7	120.4	110.2
11	1/10/26	255.1	242.8	230.8	219.1	208.2	198.6	191.6	170.5	166.8	159.4	150.3	140.5	130.4	120.1	109.7
12	1/11/26	255.2	242.8	230.7	219.1	208.1	198.4	191.3	170.8	167.0	159.4	150.2	140.2	130.0	119.7	109.3
13	1/12/26	255.3	242.9	230.7	219.0	207.9	198.1	191.0	171.1	167.1	159.3	150.0	140.0	129.7	119.4	108.9
14	1/13/26	255.4	242.9	230.7	218.9	207.8	197.9	190.7	171.4	167.2	159.3	149.8	139.8	129.5	119.0	108.6
15	1/14/26	255.5	243.0	230.7	218.8	207.6	197.6	190.3	171.7	167.4	159.3	149.7	139.5	129.2	118.7	108.2
16	1/15/26	255.6	243.0	230.7	218.7	207.4	197.4	189.9	172.1	167.5	159.3	149.6	139.3	128.9	118.3	107.8
17	1/16/26	255.7	243.1	230.7	218.7	207.3	197.1	189.5	172.5	167.7	159.3	149.4	139.1	128.6	118.0	107.4

Figure 6. Geocentric transfer angle θ values in degrees (measured from the Moon's position r_M 5 days prior to each column's Earth depart date through the transfer to TNI) are tabulated as a function of TNI date (columns) and NAI date (rows) at 1-day increments. Near-Hohmann values with $160^\circ < \theta < 200^\circ$ are green in color. Boxed dates, together with Cell I10's $\theta = 170.2^\circ$, pertain to the selected outbound mission leg selection from TNI to NAI.

The boxed cell in Figure 6 is chosen for further targeting and refinement because its θ value is very nearly the ideal 180° for NAI's 9.0 January 2026 UTC already selected from Figures 2 and 3. Heliocentric position and velocity in the Earth mean equator and equinox of epoch J2000.0

coordinate system (J2K) for 1999 AO₁₀ intercept on that date are $\mathbf{r}_{NAI} = \begin{bmatrix} -55206160.6 \\ +126166035.3 \\ +57399785.9 \end{bmatrix}$ km

Targeting Interplanetary Departures & Arrivals From The Moon

and $\mathbf{v}_{NAI+} = \begin{bmatrix} -26.936220 \\ -7.677256 \\ -4.618121 \end{bmatrix}$ km/s. A dedicated heliocentric Lambert solution is obtained for the boxed case, and it applies patched conic theory to obtain a preliminary geocentric \mathbf{v}_∞ to be imparted by TNI at 25.0 September 2025 UTC. With the TEI epoch initially set at 20.0 September UTC, a geocentric J2K $\mathbf{r}_O = \begin{bmatrix} -359916.022 \\ +130344.414 \\ +139704.668 \end{bmatrix}$ km is determined from Table 3's selenocentric EPM position.

Along with $r_P = 6778.137$ km, both \mathbf{v}_∞ and \mathbf{r}_O are input to a *cIntercept* spreadsheet performing the following operations.

- 1) Use Equation 1 to compute $\beta = 13.520^\circ$.
- 2) Negate components of \mathbf{v}_∞ to compute geocentric J2K $\mathbf{c} = \begin{bmatrix} +1.075305 \\ -0.231123 \\ -0.682937 \end{bmatrix}$ km/s according to its definition for Earth departures.
- 3) Replacing \mathbf{r}_M with \mathbf{r}_O , use Equations 3 through 7 and 8a to compute geocentric J2K $\mathbf{r}_P = \begin{bmatrix} +4963.149 \\ -196.426 \\ -4612.126 \end{bmatrix}$ km.
- 4) Use Equations 9 and 10 to compute geocentric J2K $\mathbf{v}_P = \begin{bmatrix} -5.542706 \\ +7.023833 \\ -6.263693 \end{bmatrix}$ km/s at TNI+.
- 5) Use Equations 11 through 15 with $\phi = -\beta = -13.520^\circ$ to compute geocentric J2K $\mathbf{r} = \begin{bmatrix} +5710.014 \\ -1227.292 \\ -3626.490 \end{bmatrix}$ km at *c*-intercept.¹⁸

A geocentric Long-Way Lambert transfer solution is then obtained using \mathbf{r}_O on 20.0 September UTC and \mathbf{r} at *c*-intercept on 25.0 September UTC as BCs. The solution reestablishes preliminary Figure 1 geometry for a geocentric transfer angle from \mathbf{r}_O to \mathbf{c} . This angle, inclusive of Operation 1's β , is $\theta_O = 207.2^\circ$ and is 37.0° larger than the boxed θ value defined by \mathbf{r}_M in Figure 6.

Use the TNI+ circumstances at 25.0 September 2025 UTC computed by *cIntercept* Operations 3 and 4 to seed a DC run targeting 1999 AO₁₀ arrival on 9.0 January 2026 UTC. After 20 DC

¹⁸ Note this computation of elliptical lunar transfer position at *c*-intercept assumes hyperbolic conic motion at TNI+ and is thus an approximation. Along-track position error from this approximation is small because TNI Δv is small and β , the arc between \mathbf{c} and \mathbf{r}_P , spans a short time interval.

Targeting Interplanetary Departures & Arrivals From The Moon

iterations, seeded TNI+ J2K velocity is modified to $\begin{bmatrix} -4.600576 \\ +8.323776 \\ -5.350753 \end{bmatrix}$ km/s. Although refined TNI+ velocity is still near perigee (the TNI+ trajectory has minimum height above Earth's equatorial radius $H_P = +399.9$ km and inertial flight path angle $\gamma = +0.163^\circ$), heading in the local horizontal plane has been corrected from $\psi = +141.492^\circ$ to $\psi = +131.790^\circ$ east of true north.

The large TNI+ heading correction must be reflected in a refined c . This is accomplished by input of Operation 3's r_P and the DC-refined TNI+ velocity to a $vINF$ spreadsheet as r and v , respectively. The following operations are then performed in $vINF$.

- 6) Use Equations 17 through 19 to refine $\beta = 12.669^\circ$.
- 7) Use Equations 20 through 22 and 23a to refine geocentric J2K $c = \begin{bmatrix} +0.979705 \\ -0.241948 \\ -0.670201 \end{bmatrix}$ km/s.
This correction is 2.284° from the preliminary vector supplied by heliocentric Lambert targeting.
- 8) Use Equations 24, 14, and 15 with $\phi = -\beta = -12.669^\circ$ to compute geocentric J2K $r = \begin{bmatrix} +5550.058 \\ -1370.641 \\ -3796.710 \end{bmatrix}$ km at c -intercept.

Refined geocentric transfer Lambert targeting is enabled by $vINF$ Operation 8 supplying the c -intercept position at 25.0 September UTC. The other r_O BC at 20.0 September UTC is unchanged from preliminary geocentric Lambert targeting. This Long-Way solution then seeds a DC run targeting the conic Lambert trajectory about an hour before perigee. In turn, this first DC solution seeds another targeting Operation 8's c -intercept position in the manner prescribed by Section 4.0.

The critical condition following this three-stage targeting process is $\phi = -\beta$ at c -intercept as prescribed by Figure 1 for Earth departures. With r_O at epoch 20.0 September UTC, $\phi = +15.089^\circ$ after three-stage targeting. To obtain closer conformance with the $\phi = -\beta$ condition, it is necessary to reduce θ_O by delaying TEI. Iterating three-stage targeting on TEI's epoch converges on 20 September 2025 at 05:00 UTC. With this delay, geocentric J2K $r_O = \begin{bmatrix} -368228.586 \\ +115811.320 \\ +131642.861 \end{bmatrix}$ km, $v_{TEI} = \begin{bmatrix} -0.369616 \\ -0.745664 \\ -0.434182 \end{bmatrix}$ km/s, and $\theta_O = 177.6^\circ$, only 7.4° larger than Figure 6's boxed value. The reduction in θ_O triggers transition to Short-Way geocentric Lambert targeting, and the second DC run produces $\phi = -12.929^\circ$ at c -intercept, a value 0.26° smaller than ideal.

Iterating on the TEI epoch with three-stage targeting produces the first precision transfer trajectory. With TEI on 20 September 2025 at 05:00 UTC, perigee occurs on 25 September 2025

Targeting Interplanetary Departures & Arrivals From The Moon

at 00:02:23.459 UTC, 2.4 minutes after c -intercept, with $\mathbf{r}_P = \begin{bmatrix} +6018.258 \\ -1928.811 \\ -2441.912 \end{bmatrix}$ km, $H_P = +397.0$

km, and $\psi = -14.704^\circ$. Note this transfer's inclination is marginally retrograde with respect to Earth's equator while also being marginally prograde with respect to the ecliptic and the Moon's geocentric orbit.

The c from $vINF$, together with geocentric position from the precision transfer trajectory one hour before c -intercept, are input to a $cInterceptR1$ spreadsheet to obtain geocentric J2K $\mathbf{v}_P = \begin{bmatrix} +2.823870 \\ -3.808141 \\ +9.828780 \end{bmatrix}$ km/s at TNI+ using Equation 10.

The precision transfer's \mathbf{r}_P and $cInterceptR1$'s \mathbf{v}_P estimate seed a second DC run targeting 1999 AO₁₀ intercept at \mathbf{r}_{NAI} on 9.0 January 2026 UTC. A converged solution is obtained with 3 DC iterations, producing TNI+ conditions having J2K $\mathbf{v} = \begin{bmatrix} +2.748075 \\ -3.903597 \\ +9.819250 \end{bmatrix}$ km/s, $\psi = -15.333^\circ$, and $\gamma = +0.070^\circ$. The associated TNI impulsive $\Delta v = 0.207$ km/s, 0.120 km/s of which is an out-of-plane "left" component because ψ is too northerly by 0.629° at TNI-.

To correct the transfer plane, \mathbf{r}_P and the DC-refined velocity at TNI+ are input to a $vINFr1$ spreadsheet as \mathbf{r} and \mathbf{v} , respectively. The following operations are then performed in $vINFr1$.

9) Use Equations 17 through 19 to refine $\beta = 12.981^\circ$.

10) Use Equations 20 through 22 and 23a to refine geocentric J2K $\mathbf{c} = \begin{bmatrix} +1.003705 \\ -0.243640 \\ -0.689542 \end{bmatrix}$ km/s.

This correction is 0.235° from the preliminary vector supplied by $vINF$ Operation 7.

11) Use Equations 24, 14, and 15 with $\phi = -\beta = -12.981^\circ$ to compute geocentric J2K $\mathbf{r} = \begin{bmatrix} +5550.047 \\ -1347.224 \\ -3812.860 \end{bmatrix}$ km at c -intercept.

The foregoing $vINFr1$ corrections are minute to a degree that TEI's epoch is held as 20 September 2025 at 05:00 UTC. Although \mathbf{r}_O is also unchanged, Operations 9 and 11 produce $\theta_O = 177.7^\circ$, an increase of 0.1° . Three-stage targeting then produces a perigee on 25 September 2025 at 00:02:25.626 UTC, 2.167 s later than the first precision TNI epoch. Refined TNI-

perigee conditions are $\mathbf{r}_P = \begin{bmatrix} +6020.736 \\ -1927.512 \\ -2441.713 \end{bmatrix}$ km, $\mathbf{v}_{TNI-} = \begin{bmatrix} +2.698852 \\ -3.825660 \\ +9.674789 \end{bmatrix}$ km/s, $H_P = +398.8$ km,

and $\psi = -15.261^\circ$. This refinement also produces geocentric J2K $\mathbf{v}_{TEI+} = \begin{bmatrix} +0.111300 \\ +0.049356 \\ -0.138374 \end{bmatrix}$ km/s.

The vector difference $\mathbf{v}_{TEI+} - \mathbf{v}_{TEI-}$ has magnitude equivalent to TEI $\Delta v = 0.975$ km/s.

Targeting Interplanetary Departures & Arrivals From The Moon

Targeting 1999 AO₁₀ intercept on 9.0 January 2026 UTC from the revised r_P with DC produces

TNI+ conditions having J2K $\mathbf{v}_{TNI+} = \begin{bmatrix} +2.752913 \\ -3.889993 \\ +9.821737 \end{bmatrix}$ km/s, $\psi = -15.263^\circ$, and $\gamma = +0.070^\circ$. The

vector difference $\mathbf{v}_{TNI+} - \mathbf{v}_{TNI-}$ has magnitude and associated TNI impulsive $\Delta v = 0.169$ km/s, virtually all of which is prograde. This DC run also produces a heliocentric J2K $\mathbf{v}_{NAI-} =$

$\begin{bmatrix} -28.678418 \\ -9.038157 \\ -4.163670 \end{bmatrix}$ km/s. The $\mathbf{v}_{NAI+} - \mathbf{v}_{NAI-}$ vector difference has magnitude equivalent to NAI $\Delta v = 2.257$ km/s.

It should be noted final three-stage targeting obtains $\phi = -13.118^\circ$ at c -intercept, 0.137° more negative than desired. Furthermore, $\phi = -13.118^\circ$ appears very near a local maximum with TEI epoch variations, and the desired value cannot be attained to better than 0.1° precision. When TNI is moved to 26.0 September 2025 UTC, the associated ϕ shortfall becomes 1.925° . In these shortfall cases, perigee falls beyond c -intercept such that it lies outside the LPIP. If this geometry cannot otherwise be corrected, it is addressed by moving TNI earlier. In the 26.0 September case, moving TNI to 25 September at 23:53 UTC has a nearly minimal $\Delta v = 0.172$ km/s. The $\phi = -\beta$ condition is easily achieved when TNI is moved to circa 24.0 September UTC. These results are summarized in Table 4.

Table 4. The precision with which Figure 1 geometry can be targeted is summarized for three consecutive TNI dates in late September 2025. As the TEI-to-TNI geocentric transfer angle θ_0 approaches 180° , transfer targeting nears a singularity at which any transfer plane is possible. True anomaly ϕ applies to position at c -intercept, a byproduct of three-stage TEI-to-TNI targeting. By virtue of c -intercept targeting, TNI Δv has a negligible out-of-plane component for all three cases. In contrast, non-zero $\phi + \beta$ can introduce an appreciable TNI Δv radial component (positive downward) as tabulated in the rightmost column.

TNI Date	θ_0 (deg)	$\phi + \beta$ (deg)	TNI Δv (km/s)	TNI Δv_{RAD} (km/s)
09/24/2025	177.5	+0.005	0.167	+0.001
09/25/2025	177.7	-0.137	0.169	-0.013
09/26/2025	178.2	-1.925	0.172	+0.033

The targeted geocentric trajectory for TNI circa 25.0 September UTC, together with that for the Moon, is plotted from TEI to about a day after TNI in Figure 7. A noteworthy feature of this plot is perigee and TNI in Earth's shadow cast by the Sun. Total solar obscuration lasts for nearly 20 minutes, beginning 24 September at 23:55:00 UTC and ending 25 September at 00:14:42 UTC. Mission impacts such an eclipse would pose remain to be identified, but total and continuous reliance on critical solar-powered systems is inadvisable for HSF missions relying on low-altitude powered flybys. At NEO destinations, it may be essential to spend hours or days in the object's shadow to protect the crew from exposure to solar radiation.

Targeting Interplanetary Departures & Arrivals From The Moon

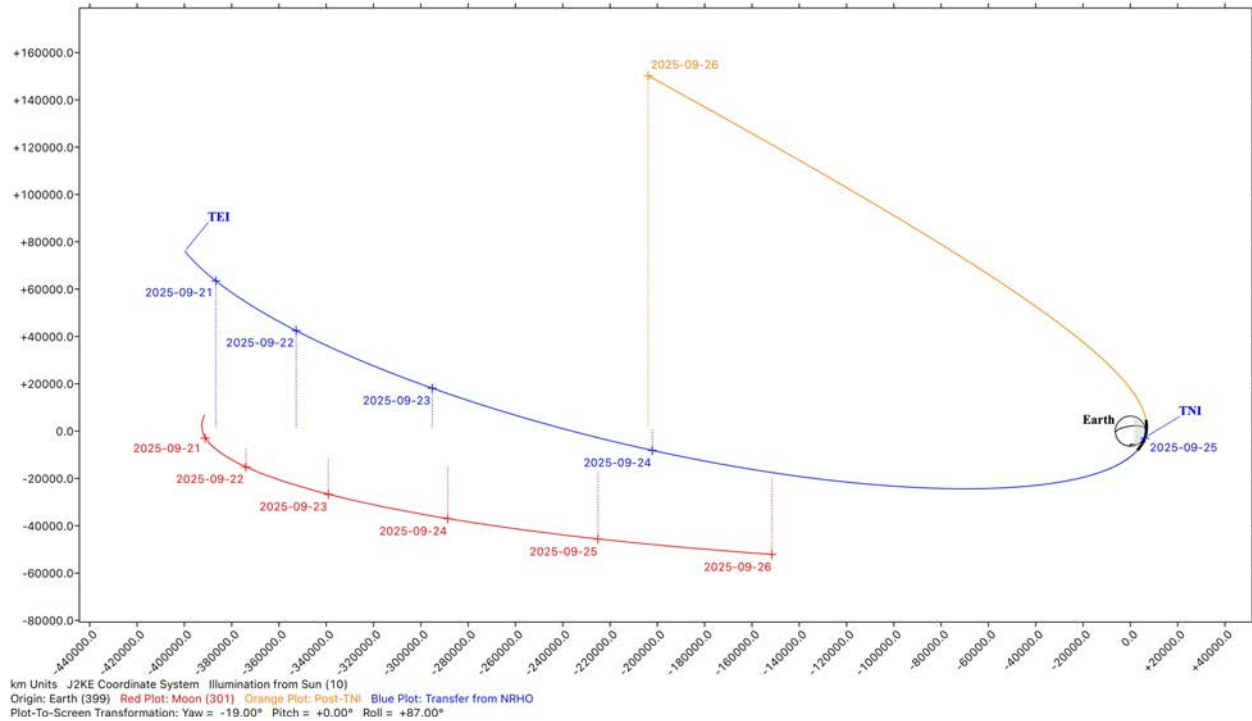


Figure 7. Inertial geocentric motion for the Moon (red) is coplotted with targeted transfer from TEI to TNI (blue) and targeted Earth departure bound for 1999 AO₁₀ post-TNI (orange). These loci are viewed from a perspective roughly normal to the targeted trajectory plane, considerably foreshortening the Moon's orbit. Dotted lines are projections onto the ecliptic plane from daily "+" markers annotated with the date in YYYY-MM-DD format at 00:00 UTC. The black trajectory arc spanning TNI lies within Earth's shadow, and the area shaded gray is Earth's nightside.

5.4 Example Targeting NDI, TLI, And LOI Following 1999 AO₁₀ Loiter

Figure 8 is a PCC tabulating θ values at daily intervals as reckoned by return heliocentric Short-Way Lambert targeting from NDI to TLI. Color-coded θ intervals form horizontal bands in this PCC because each row is 5 days before a potential LOI date and therefore corresponds to a specific lunar geocentric position \mathbf{r}_M .

The boxed cell in Figure 8 is chosen for further targeting and refinement because its θ value is very nearly the ideal 180° for NDI's 19.0 January 2026 UTC already selected from Figures 4 and

5. Heliocentric J2K position for 1999 AO₁₀ departure on that date is $\mathbf{r}_{NDI} = \begin{bmatrix} -77549157.9 \\ +117705614.0 \\ +52582615.4 \end{bmatrix}$

km. A dedicated Short-Way heliocentric Lambert solution is obtained for the boxed case with

$\mathbf{v}_{NDI+} = \begin{bmatrix} -24.538486 \\ -13.336394 \\ -6.159522 \end{bmatrix}$ km/s, and it applies patched conic theory to obtain a preliminary

geocentric J2K \mathbf{v}_∞ to be in effect for Earth return at 28.0 February 2026 UTC. With the LOI

Targeting Interplanetary Departures & Arrivals From The Moon

epoch now set at 5.0 March UTC, a geocentric J2K $\mathbf{r}_O = \begin{bmatrix} -396768.970 \\ -25538.965 \\ +48238.232 \end{bmatrix}$ km is determined from Table 3's selenocentric EPM position.

	A	B	C	D	E	F	G	H	I	J	K	L	M	N	O	P
1	Earth															
2	Return Date	1/12/26	1/13/26	1/14/26	1/15/26	1/16/26	1/17/26	1/18/26	1/19/26	1/20/26	1/21/26	1/22/26	1/23/26	1/24/26	1/25/26	1/26/26
3	2/21/26	102.0	102.4	102.9	103.4	103.9	104.5	105.1	105.8	106.6	107.4	108.3	109.2	110.3	111.4	112.6
4	2/22/26	114.5	115.0	115.4	116.0	116.5	117.1	117.8	118.5	119.3	120.1	121.0	122.0	123.0	124.2	125.4
5	2/23/26	127.0	127.4	127.9	128.5	129.1	129.7	130.4	131.1	131.9	132.8	133.7	134.7	135.8	137.0	138.2
6	2/24/26	139.2	139.7	140.3	140.8	141.5	142.1	142.8	143.6	144.4	145.3	146.3	147.3	148.4	149.6	151.0
7	2/25/26	151.2	151.7	152.3	152.9	153.5	154.2	155.0	155.8	156.7	157.6	158.6	159.7	160.9	162.1	163.5
8	2/26/26	162.5	163.1	163.7	164.3	165.0	165.8	166.6	167.4	168.3	169.3	170.4	171.5	172.8	174.1	175.5
9	2/27/26	172.6	173.2	173.9	174.5	175.3	176.1	176.9	177.8	178.8	179.8	181.0	182.2	183.5	184.9	186.5
10	2/28/26	180.1	180.7	181.3	181.9	182.6	183.3	184.1	184.9	185.7	186.6	187.6	188.6	189.6	190.6	192.1
11	3/1/26	178.0	177.7	177.4	177.1	176.8	176.5	176.2	176.0	175.8	175.6	175.6	175.6	175.7	176.0	176.4
12	3/2/26	182.8	182.9	183.0	183.1	183.3	183.5	183.7	184.0	184.3	184.7	185.2	185.8	186.4	187.1	188.0
13	3/3/26	191.5	191.8	192.1	192.5	192.9	193.4	193.9	194.4	195.0	195.7	196.4	197.2	198.1	199.0	200.1
14	3/4/26	201.6	202.0	202.5	203.0	203.6	204.2	204.8	205.5	206.3	207.1	207.9	208.9	209.9	210.9	212.1
15	3/5/26	212.2	212.7	213.3	213.9	214.6	215.3	216.0	216.8	217.6	218.5	219.5	220.5	221.6	222.8	224.0
16	3/6/26	223.0	223.6	224.3	225.0	225.7	226.5	227.3	228.2	229.1	230.1	231.1	232.2	233.4	234.6	235.9
17	3/7/26	234.0	234.7	235.4	236.2	236.9	237.8	238.7	239.6	240.6	241.6	242.7	243.9	245.1	246.4	247.8

Figure 8. Geocentric transfer angle θ values in degrees (measured from TLI to the Moon's position \mathbf{r}_M 5 days after each row's Earth return date) are tabulated as a function of NDI date (columns) and TLI date (rows) at 1-day increments. Near-Hohmann values with $160^\circ < \theta < 200^\circ$ are green in color. Boxed dates, together with Cell I10's $\theta = 184.9^\circ$, pertain to the selected return mission leg selection from NDI to TLI.

Along with $r_P = 6778.137$ km, both \mathbf{v}_∞ and \mathbf{r}_O are input to a *cIntercept* spreadsheet performing the following operations.

- 1) Use Equation 1 to compute $\beta = 21.196^\circ$.
- 2) Equate components of \mathbf{v}_∞ to compute geocentric J2K $\mathbf{c} = \begin{bmatrix} +1.988441 \\ +0.484777 \\ -0.279430 \end{bmatrix}$ km/s according to its definition for Earth returns.
- 3) Replacing \mathbf{r}_M with \mathbf{r}_O , use Equations 3 through 7 and 8b to compute geocentric J2K $\mathbf{r}_P = \begin{bmatrix} +6686.183 \\ -885.389 \\ -673.933 \end{bmatrix}$ km.
- 4) Use Equations 9 and 10 to compute geocentric J2K $\mathbf{v}_P = \begin{bmatrix} +1.310317 \\ +10.884569 \\ -1.299918 \end{bmatrix}$ km/s at TLI-.
- 5) Use Equations 11 through 16 with $\phi = \beta = +21.196^\circ$ to compute geocentric J2K $\mathbf{r} = \begin{bmatrix} +6761.443 \\ +1648.422 \\ -950.167 \end{bmatrix}$ km and $\mathbf{v} = \begin{bmatrix} -0.632251 \\ +10.780856 \\ -1.065998 \end{bmatrix}$ km/s at *c*-intercept.¹⁹

¹⁹ Note this computation of elliptical lunar transfer position at *c*-intercept assumes hyperbolic conic motion at TLI+ and is thus an approximation. Along-track position error from this approximation is small because TLI Δv is small and β , the arc between \mathbf{r}_P and \mathbf{c} , spans a short time interval.

Targeting Interplanetary Departures & Arrivals From The Moon

Initialize a geocentric Earth return ephemeris with the position and velocity computed in Operation 5, coasting backward in time to span the interval from 26.0 February UTC to 28.0 February UTC at c -intercept. Perform an initial DC run seeded with the heliocentric Lambert solution's \mathbf{r}_{NDI+} and \mathbf{v}_{NDI+} , targeting position in the Earth return ephemeris at 26.0 February UTC with a geocentric distance of 500,741.7 km. The first DC run converges in 3 iterations and seeds a second targeting Earth return ephemeris position on 27 February at 23:00 UTC with a geocentric distance of 23,356.0 km. This second DC run converges in 4 iterations and seeds a third targeting perigee in the Earth return ephemeris on 27 February at 23:56:06.832 UTC. After

2 iterations, this DC run converges to heliocentric J2K $\mathbf{v}_{NDI+} = \begin{bmatrix} -24.620222 \\ -13.373787 \\ -6.148174 \end{bmatrix}$ km/s with a refined $\mathbf{r}_{TLI} = \begin{bmatrix} +6683.834 \\ -891.618 \\ -672.927 \end{bmatrix}$ km and $\mathbf{v}_{TLI-} = \begin{bmatrix} +1.196649 \\ +10.886574 \\ -1.218349 \end{bmatrix}$ km/s. These near-perigee conditions have $\psi = +96.429^\circ$, $\gamma = -0.682^\circ$, and $H_P = +397.5$ km.

When the 3-DC-targeted \mathbf{r}_{TLI} and \mathbf{v}_{TLI-} are input to a $vINF$ spreadsheet as \mathbf{r} and \mathbf{v} , respectively, the following operations are then performed.

6) Use Equations 17 through 19 to refine $\beta = 20.046^\circ$.

7) Use Equations 20 through 22 and 23b to refine geocentric J2K $\mathbf{c} = \begin{bmatrix} +1.874135 \\ +0.461325 \\ -0.259386 \end{bmatrix}$ km/s. This correction is 0.174° from the preliminary vector supplied by heliocentric Lambert targeting.

8) Use Equations 24, 14, and 15 with $\phi = \beta = +20.046^\circ$ to compute geocentric J2K $\mathbf{r} = \begin{bmatrix} +6733.364 \\ +1657.442 \\ -931.918 \end{bmatrix}$ km at c -intercept.

A geocentric Short-Way Lambert transfer solution is obtained from Operation 8's c -intercept position at 28.0 February UTC and targeting \mathbf{r}_O at 5.0 March UTC with $\theta_O = 190.0^\circ$, 5.1° larger than the boxed value in Figure 8. When this solution seeds a corresponding DC run, it converges

in 4 iterations. Conditions at c -intercept are J2K $\mathbf{v} = \begin{bmatrix} -1.945399 \\ +10.367056 \\ -0.883771 \end{bmatrix}$ km/s, $\phi = +7.729^\circ$, and $H_P = +587.3$ km.

The $\phi \neq \beta$ mismatch from DC transfer targeting indicates a 5.0 March UTC LOI epoch is too late. This triggers LOI epoch iterations converging on 3 March at 17:00 UTC with geocentric

J2K $\mathbf{r}_O = \begin{bmatrix} -376396.343 \\ +75278.901 \\ +102972.100 \end{bmatrix}$ km and $\mathbf{v}_{LOI+} = \begin{bmatrix} -0.272905 \\ -0.798329 \\ -0.461280 \end{bmatrix}$ km/s. Reducing Δt_X by 31 hours

Targeting Interplanetary Departures & Arrivals From The Moon

results in DC-targeted c -intercept conditions becoming $\mathbf{v} = \begin{bmatrix} -0.123860 \\ +10.050978 \\ +3.338311 \end{bmatrix}$ km/s, $\phi = +20.065^\circ$, and $H_P = +409.4$ km.

A geocentric Earth return ephemeris is then initialized with the foregoing c -intercept conditions at 28.0 February UTC and coasted to span the UTC interval from 27.0 February to 1.0 March.

The J2K position from this ephemeris on 28 February at 01:00 UTC with $\mathbf{r} = \begin{bmatrix} -7370.006 \\ +21406.816 \\ +8667.984 \end{bmatrix}$ km is entered into a *cInterceptRI* spreadsheet, together with the \mathbf{c} vector obtained in Operation 7, thus defining a refined transfer plane. This spreadsheet performs the ensuing operation.

- 9) Use Equations 11 through 16 with $\phi = \beta = +20.046^\circ$ to compute geocentric J2K $\mathbf{r} = \begin{bmatrix} +6733.366 \\ +1657.442 \\ -931.919 \end{bmatrix}$ km and $\mathbf{v} = \begin{bmatrix} -0.041628 \\ +10.303070 \\ +3.402508 \end{bmatrix}$ km/s at c -intercept.

Operation 9's c -intercept state vector at 28.0 February UTC defines $\theta_0 = 174.3^\circ$ and initializes a geocentric Earth return ephemeris coasted from 26.0 February to 1.0 March UTC. Perigee

circumstances in this ephemeris are 27 February at 23:56:19.628 UTC, $\mathbf{r}_P = \begin{bmatrix} +6542.138 \\ -639.498 \\ -1646.360 \end{bmatrix}$ km,

$\psi = +73.436^\circ$, and $H_P = +398.2$ km. A DC run seeded by \mathbf{r}_{NDI} and the last DC-refined \mathbf{v}_{NDI+} next targets this refined UTC and \mathbf{r}_P . After 20 iterations, the DC run converges on heliocentric J2K

$\mathbf{v}_{NDI+} = \begin{bmatrix} -24.621032 \\ -13.373246 \\ -6.152779 \end{bmatrix}$ km/s to obtain near-perigee TLI- circumstances having geocentric J2K $\mathbf{v}_{TLI-} = \begin{bmatrix} +1.772536 \\ +10.456346 \\ +2.993153 \end{bmatrix}$ km/s, $\psi = +73.729^\circ$, and $\gamma = -0.014^\circ$. With $\mathbf{v}_{NDI-} = \begin{bmatrix} -24.665722 \\ -11.841667 \\ -6.497587 \end{bmatrix}$

km/s from JPL's 1999 AO₁₀ ephemeris, the vector difference $\mathbf{v}_{NDI+} - \mathbf{v}_{NDI-}$ produces NDI $\Delta v = 1.571$ km/s from its magnitude, in close agreement with the Lambert-targeted boxed value in Figure 4.

These near-perigee circumstances then seed a DC run targeting \mathbf{r}_O on 3 March at 17:00 UTC.

After 25 iterations, this processing produces TLI+ circumstances $\mathbf{v}_{TLI+} = \begin{bmatrix} +1.745987 \\ +10.196398 \\ +2.978220 \end{bmatrix}$ km/s

$\psi = +73.415^\circ$, and $\gamma = -0.001^\circ$. The vector difference $\mathbf{v}_{TLI+} - \mathbf{v}_{TLI-}$ has a magnitude equivalent to

TLI $\Delta v = 0.262$ km/s. This DC solution also determines geocentric J2K $\mathbf{v}_{LOI-} = \begin{bmatrix} -0.462211 \\ -0.008769 \\ +0.010997 \end{bmatrix}$

km/s, and the vector difference $\mathbf{v}_{LOI+} - \mathbf{v}_{LOI-}$ yields a magnitude for LOI $\Delta v = 0.939$ km/s.

The targeted geocentric trajectory for 1999 AO₁₀ return to Earth circa 28.0 February 2026 UTC, together with that for the Moon, is plotted from about a day before TLI to LOI in Figure 9.

Targeting Interplanetary Departures & Arrivals From The Moon

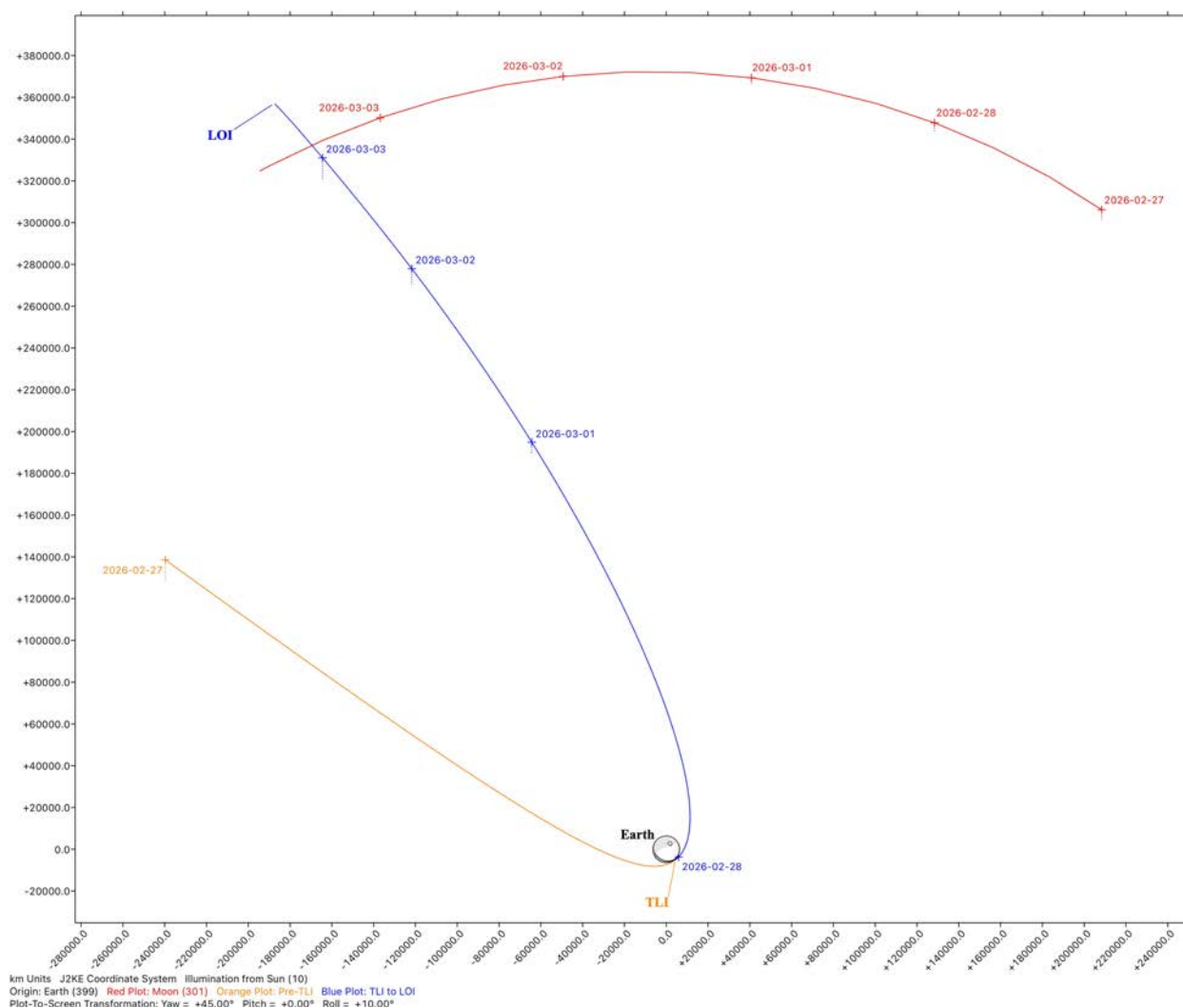


Figure 9. Inertial geocentric motion for the Moon (red) is coplotted with targeted Earth return from 1999 AO₁₀ pre-TLI (orange) and transfer from TLI to LOI (blue). These loci are viewed from a perspective roughly normal to the targeted trajectory plane. Dotted lines are projections onto the ecliptic plane from daily "+" markers annotated with the date in YYYY-MM-DD format at 00:00 UTC. The area shaded gray is Earth's nightside.

5.5 Targeting Examples Summary

The sequence of events targeted in Sections 5.3 and 5.4 appears in Table 5. A geocentric plot of this roundtrip trajectory from TNI to TLI appears in Figure 10. This plot omits TEI-to-TNI and TLI-to-LOI transfers in the interest of minimizing clutter near the origin.

Table 5. Events defined in Table 1 are summarized for the roundtrip to NEO 1999 AO₁₀ as targeted in the previous two sections. Mission Elapsed Time (MET) is the time interval in decimal days since TEI. Total Δv for this roundtrip is 6.173 km/s.

Event	UTC Date	MET (days)	Δv (km/s)
TEI	20.208 Sep 2025	0.000	0.975
TNI	25.002 Sep 2025	4.793	0.169
NAI	09.000 Jan 2026	110.792	2.257
NDI	19.000 Jan 2026	120.792	1.571
TLI	27.997 Feb 2026	160.789	0.262
LOI	03.708 Mar 2026	164.500	0.939

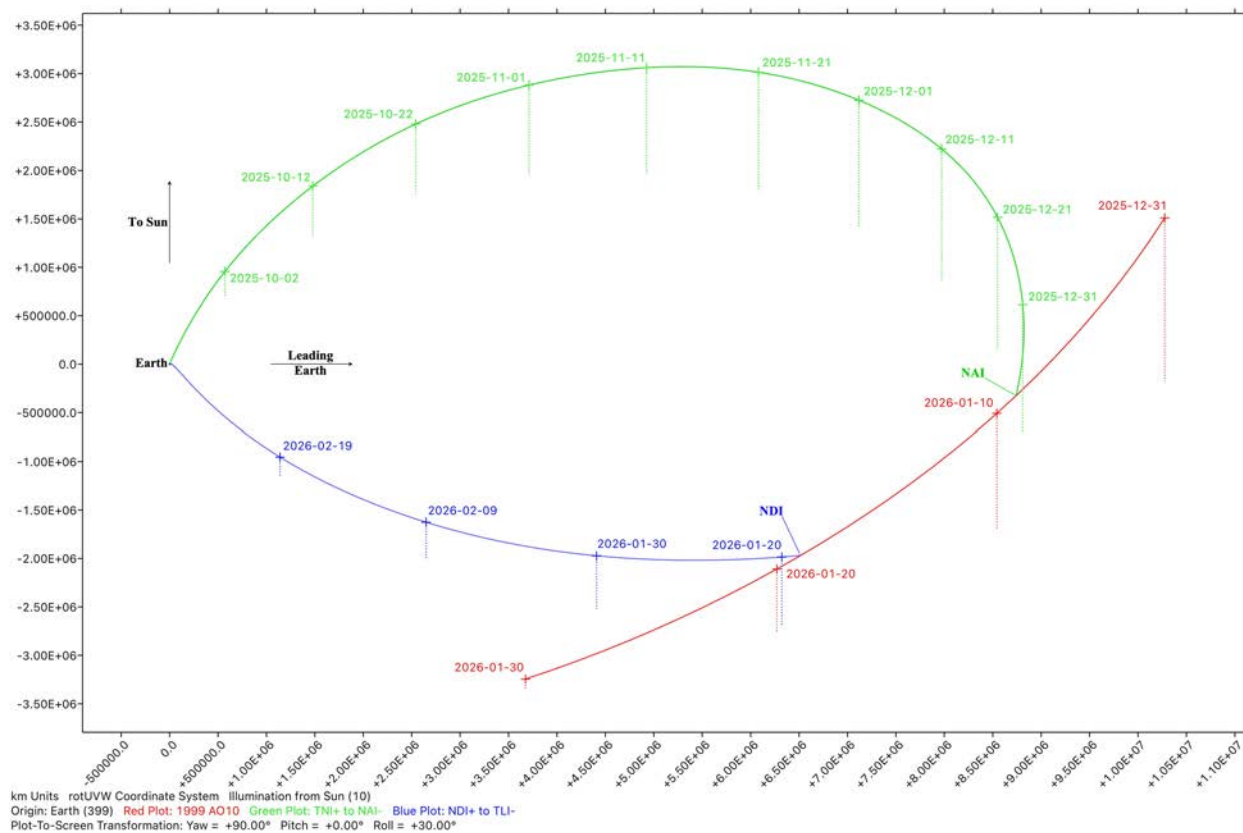


Figure 10. The 5.5-month roundtrip trajectory from Earth (at left) to 1999 AO₁₀ (**red**) is plotted in a geocentric coordinate system rotating with the Sun/Earth line. Outbound motion (**green**) gives way to a 10-day loiter at 1999 AO₁₀ before return motion (**blue**) is initiated. Appearing at 10-day intervals, "+" markers are annotated with the date in YYYY-MM-DD format at 00:00 UTC. Dotted lines from these markers are projections onto the ecliptic plane.

In Figure 10, note how the outbound leg departs Earth roughly in the Sun's direction. Because the associated powered Earth flyby in Figure 7 is a tight hairpin turn, TEI must be with the Moon in that direction too. Indeed, the Moon's phase at TEI is a waning crescent 18.2° before new.

Targeting Interplanetary Departures & Arrivals From The Moon

The return leg approaches Earth from a direction nearly opposite departure, and LOI occurs with the Moon at waning gibbous phase 3.3° past full.²⁰

Another noteworthy feature in Figure 10 is 1999 AO₁₀ approach to its descending node on the ecliptic plane as 2025 ends and 2026 begins. At NDI, 1999 AO₁₀ is only about half as far from the ecliptic as at NAI (reference dotted **red** projection lines). Consequently, excursions from the ecliptic are far less on the return leg of the roundtrip trajectory compared to the outbound leg. Since the Moon orbits Earth within 5° of the ecliptic, difficulties obtaining the desired transfer trajectory ϕ at c -intercept are greatly reduced on Earth return with respect to departure. As a measure of these difficulties, consider δ_c , the declination of c with respect to the Moon's orbit plane, computed using Equation 25.

$$\delta_c = \text{acos}\left(\frac{\mathbf{h} \cdot \mathbf{c}}{hc}\right) \quad (25)$$

Whereas the outbound leg in Figure 10 has $\delta_c = -23.2^\circ$, the return leg is favored with $\delta_c = -15.2^\circ$. Considering the interval between NAI and NDI is only 10 days, δ_c is highly dynamic with respect to destination loiter time in Figure 10.

6.0 Conclusions

Procedures with which to target interplanetary trajectories departing from and returning to the Moon's vicinity have been documented and demonstrated herein. This process makes use of patched conic theory in two contexts. First, geocentric asymptotic velocity \mathbf{v}_∞ and asymptote angle β are inferred from a heliocentric Lambert trajectory solution connecting Earth with an interplanetary destination. As illustrated in Figure 1, these two parameters then serve as boundary conditions for the second context in which hyperbolic perigee conditions are patched with those of a near-Hohmann transfer ellipse whose apogee is proximal to the Moon.

The geocentric transfer angle θ between the Moon's center and powered Earth flyby perigee has been demonstrated to be a useful metric for selecting viable departure and return dates at selenocentric altitudes near 70,000 km over transit times near 5 days. Per PCC examples in Figures 6 and 8, $160^\circ \leq \theta \leq 200^\circ$ appears to be a good preliminary viability criterion for near-Hohmann transfers. Additional analysis, including roundtrips to less accessible destinations than 1999 AO₁₀, is necessary to refine practical θ limits, however.

The validity of this paper's trajectory targeting examples is demonstrated by introducing Earth, Sun, and Moon gravity perturbations and computing DC solutions in their presence. These DC runs are often rapidly convergent when seeded by an analytic Lambert solution with similar BCs. When penetrating deep into a gravity field, such as the $H_p = +400$ km perigees at TNI and TLI targeted herein, a reference trajectory (even one with a conic pedigree) can supply intermediate positions/epochs serving as BCs to speed DC convergence. Such an intermediate solution then seeds a DC run targeting a closer position or one at perigee.

²⁰ Lunar phase angles are approximate and use elongation from the Sun/Earth line as a proxy value.

Targeting Interplanetary Departures & Arrivals From The Moon

Finally, it is hoped methods documented by this paper will prove useful in priming trajectory optimization programs with a baseline design on a particular timeline. Each baseline can then give rise to an entire family of related designs as the timeline is incremented in a manner akin to departure and arrival dates in a PCC dataset.

AIAA National Journals

<https://www.aiaa.org/publications/journals>



<https://arc.aiaa.org/journal/aiaaj>



<https://arc.aiaa.org/journal/jat>



<https://arc.aiaa.org/journal/jais>



<https://arc.aiaa.org/journal/ja>



<https://arc.aiaa.org/journal/jgcd>



<https://arc.aiaa.org/journal/jpp>



<https://arc.aiaa.org/journal/jsr>



<https://arc.aiaa.org/journal/jtht>

50+ Years of AIAA Journal Archives Online

Current and back issues of AIAA journals are available online in Aerospace Research Central (ARC).

- **AIAA Journal (1963–current):** This online-only journal was launched along with AIAA in 1963, covering pioneering theoretical developments and experimental results across a far-reaching range of disciplines.
- **Journal of Air Transportation (2016–current):** AIAA's newest online-only journal was originally published as Air Traffic Control quarterly and is devoted to new developments in air traffic management and aviation operations of all flight vehicles, including unmanned aerial vehicles (UAVs) and space vehicles, operating in the global airspace system. The scope of the journal includes theory, applications, technologies, operations, economics, and policy.
- **Journal of Aerospace Information Systems (2004–current):** This online-only journal (formerly known as the Journal of Aerospace Computing, Information, and Communication) describes new theoretical developments, novel applications, and case studies of advances in aerospace computing, information, and communication systems.
- **Journal of Aircraft (1964–current):** Focusing on major advances in aircraft technology, this journal covers major development in general aviation, military and civilian aircraft, STOL and V/STOL aircraft, subsonic, supersonic, transonic, and hypersonic aircraft as well as applications on aircraft technology to related fields.
- **Journal of Energy (1977–1983):** You can now retrieve papers from this archived journal that was devoted to advancing the knowledge of terrestrial and space applications of all forms of energy, including its production, transformation, and conservation. propulsion, plus power generation and conversion, and terrestrial energy systems in the Journal of Propulsion and Power.

AIAA National Journals

<https://www.aiaa.org/publications/journals>

- Journal of Guidance, Control, and Dynamics (1978–current): Keep pace with recent research and practical engineering applications that are guiding new generations of high-performance air and space vehicles — both manned and. This journal was originally published as the Journal of Guidance and Control.
- Journal of Hydronautics (1967–1980): Access archived articles from this retired journal to explore theoretical and experimental knowledge of hydrodynamics, including propulsion systems and the design of underwater vehicles, highlighting the intersection between ocean and aerospace science and engineering.
- Journal of Propulsion and Power (1985–current): Discover advances in air-breathing, electric, and advanced propulsion, plus power generation and conversion, and terrestrial energy systems in the Journal of Propulsion and Power.
- Journal of Spacecraft and Rockets (1964–current): This journal features the best new work in spacecraft and missile systems (tactical and strategic), including subsystems, applications, missions, environmental interactions, and space sciences.
- Journal of Thermophysics and Heat Transfer (1987–current): Explore the latest developments in thermal energy transfer and storage — in gases, liquids, and solids.

Out of the Past: AIAA's Predecessor Society Journal Archives

Archive copies from AIAA's predecessor society publications also are available online in ARC.

- Bulletin of the American Interplanetary Society (1930–1932): This bimonthly newsletter of the American Interplanetary Society (later known as the American Rocket Society) shared the wonders of space travel with the fledgling society's members.
- Astronautics (1932–1944): Published monthly by the American Interplanetary Society, this formal newsletter replaced the Bulletin of the American Interplanetary Society.
- Journal of the Aeronautical Sciences(1934–1957) and Journal of the Aerospace Sciences (1958-1962): The monthly journal of the Institute of the Aeronautical Science (later the Institute of the Aerospace Sciences) published scientific and technical articles along with member news.
- Journal of the American Rocket Society (1945-1953): This journal published technical articles on experiments in rocketry and scientific research and engineering development of jet propulsion devices and their application to problems of transportation and communication.
- Journal of Jet Propulsion (1954–1958): This journal published by the American Rocket Society was devoted to the advancement of the field of jet propulsion through the publication of original scientific papers and also shared society news.
- ARS Journal (1959–1962): Originally published under the title Journal of Jet Propulsion the name change of this journal reflected the ever-broadening field of interest of the American Rocket Society. Papers were chosen for publication based on their pertinence to the general field of astronautics, the future significance of the research, and importance to the members of the society and the profession at large.

AIAA National 2023 Fall Course Catalog Released



Build Skills with Online Courses

The Institute is offering 16 online short courses this fall to help you stay sharp and improve your knowledge base. These courses are taught by renowned industry leaders and experts. Special pricing is available for AIAA members and student members, as well as group discounts for five or more individuals from the same organization. Enroll in an upcoming course.

BROWSE CATALOG

UPCOMING COURSES



Foundations of Digital Engineering

Starts 11 September

Enroll Now



Fundamentals of Space Domain Awareness

Starts 12 September

Enroll Now

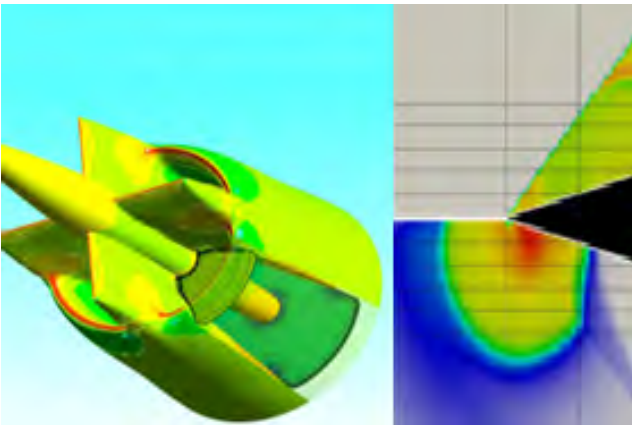
AIAA National 2023 Fall Course Catalog Released



Spacecraft Design, Development, and Operations
Starts 18 September
Enroll Now



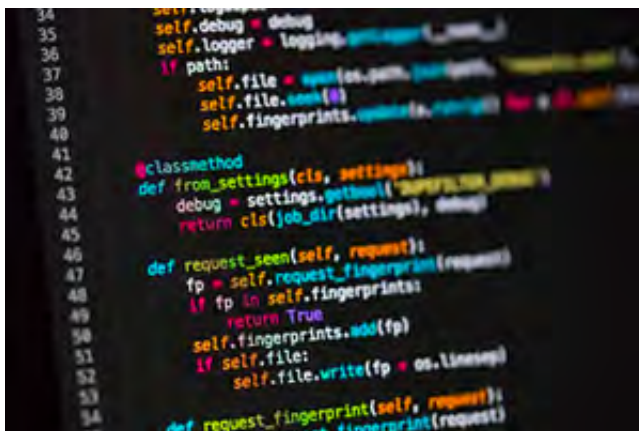
Aircraft Reliability and Reliability Centered Maintenance
Starts 19 September
Enroll Now



Fundamentals of High Speed Air-Breathing
and Space Propulsion
Starts 19 September
Enroll Now



Flight Dynamics and Control of Aircraft,
Missiles, and Hypersonic Vehicles
Starts 26 September
Enroll Now



Overview of Python for Engineering
Programming
Starts 2 October Enroll Now



Metal Additive Manufacturing for Aerospace Applications
Starts 10 October
Enroll Now

AIAA National 2023 Fall Course Catalog Released



Applied Model-Based Systems Engineering
Starts 10 October
Enroll Now



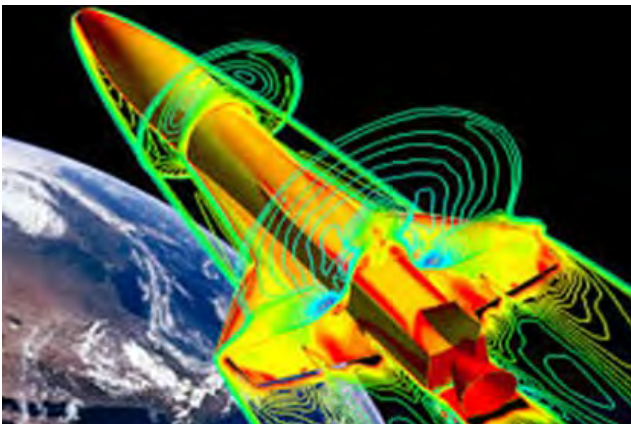
Space Domain Cybersecurity
Starts 16 October
Enroll Now



Wind Tunnel Testing for Aircraft Development
Starts 17 October
Enroll Now



Technical Writing Essentials for Engineers
Starts 24 October
Enroll Now



Hypersonic Applications: Physical Models for
Interdisciplinary Simulation
Starts 30 October
Enroll Now



Space Architecture: Designing an Orbital
Habitation System
Starts 31 October
Enroll Now

AIAA National 2023 Fall Course Catalog Released



Business Development for
Aerospace Professionals
Starts 7 November
Enroll Now



Aircraft and Rotorcraft System ID with
CIFER
Starts 4 December
Enroll Now

Announcement: AIAA Email notices frequency adjustment

Please contact us:
contact@aiaa-lalv.org

- Reduce the email notices: if you feel you are getting too many emails from AAA LA-LV Section, please don't unsubscribe. We can adjust the frequency of the emails for you.
- Increase frequencies if you would like to receive our emails more often or all email notices from us.
- Too busy and forgot to renew membership? Want to receive membership reminder emails or calls from AIAA LA-LV Section? Please contact us. Continuously paying the membership dues will lead to potential emeritus membership status after 50 years with no more dues to pay afterwards. Please take a look here also for other membership dues discounts etc., like Young Professional (35 years old or under, above college), Retiree, and more. <https://www.aiaa.org/membership/join-or-renew-your-aiaa-membership/Membership-Dues>

Announcement: Resources of Career Opportunities

AIAA LA-LV Section Career Resources

<https://www.aiaa-lalv.org/career>

<https://engage.aiaa.org/losangeles-lasvegas/viewdocument/career-job-and-internship-web-lin>

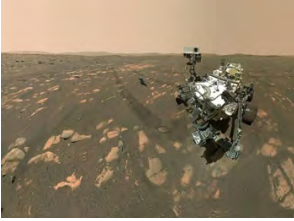

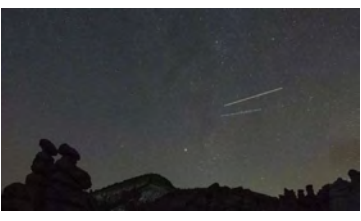
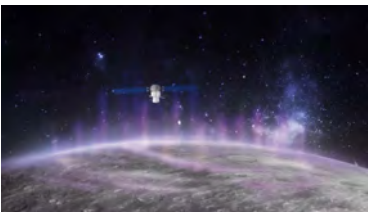
















Job Seekers:

The [AIAA Career Center Job Board](#) is free for members looking for new opportunities - post a resume, get alerts based on your interests. You might also want to check out:

- [Meet the Employers @ AVIATION 2023 \(June 2023\)](#)
- [AIAA Professional Virtual Career Fair \(Sept 2023\)](#)

Recruiters: find the best candidates by searching resumes on the AIAA Job Board or participating in Meet-the-Employer sessions and Career Fairs

- [Post a Job through the Career Center](#)
- [Meet the Employers @ AVIATION 2023](#)
- [Professional Virtual Career Fair \(Sept 2023\)](#)

			
(July 17) Senate Unveils Flat NASA Budget, Takes Aim at Mars Sample Return	(July 19) 'Space junk' seen over Wellington believed to be Elon Musk satellite	(July 18) 'Meteorite' that struck French woman was just a regular Earth rock, experts say	(July 18) Auroras across the solar system are powered in the same way, Mercury results suggest
			
(July 17) DARPA taps Raytheon for next phase of air-breathing hypersonic program	(July 18) Venezuela signs up to China's moon base initiative	(July 13) 'Stargazer', the new hypersonic jet that will take you from Tokyo to San Francisco in an hour	(July 14) The UK will send Eurofighter Typhoon FGR4 fighter jets to Finland to test the ability to take off and land on a motorway track
			
(July 13) General Officer Announcements (Space Force / DoD)	(July 20) Anduril has won 10.5 million in Small Business Innovation Research contracts for its Lattice networking software	(July 16) Virgin Galactic's second commercial spaceflight is underway	(July 18) James Webb Space Telescope starts in new Netflix documentary 'Unknown: Cosmic Time Machine' (exclusive trailer)
			
(July 15) Last chances in 2023 to see comets from home without using a telescope	(July 13) Senate defense panel leaves National Security Space Launch unsecured	(July 13) A new, thin-lensed telescope design could far surpass James Webb	(June 30) Why People Are Worried Virgin Galactic Will Be The Next Titan Sub
			
(July 2) Advances in Rocket Propulsion Will Thrust America Past China's Space Program	(July 11) Virgin Group has decided not to buy 'Overture' supersonic jets	(June 5) GEO satellite outage speaks to the value of Iridium LEO mesh network	(July 10) IMPOSSIBLE QUANTUM DRIVE THAT DEFIES KNOWN LAWS OF PHYSICS SCHEDULED FOR "DO OR DIE" OCTOBER SPACE FLIGHT

RSVP and Information: (<https://conta.cc/44mE7A9>)

AIAA LA-LV 8/5 Section (Hybrid) Meeting

Saturday, August 5, **11 AM PDT** (US and Canada) (GMT -0700)

Special Lecture in Aerospace Geoengineering to Mitigate Climate Change – Is there a Role for Aerospace?

Lecturer

Dr. Marty Bradley

AIAA Fellow

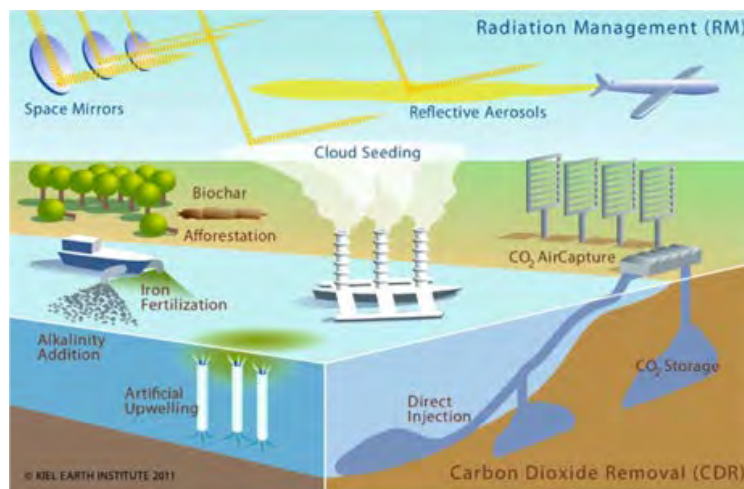
Sustainable Aviation Consultant & Fellow of the AIAA

Adjunct Professor of Aerospace and Mechanical Engineering Practice at USC

Senior Technical Fellow for electric aircraft and sustainability at Electra.aero

Retired Boeing Technical Fellow for advanced technology concepts and propulsion

(The speaker will present in person.)



Physical Location

Culver City Julian Dixon Library, Meeting Room
4975 Overland Ave, Culver City, CA 90230

(South of Hwy 10, North / East of Hwy 405, and West of Hwy 110)
(Library parking is available, plus other possible street parking. Please follow the signs.) (This event is not sponsored by the Culver City Julian Dixon Library)

Online on Zoom

(Please register /RSVP and you will receive the ticket with the Zoom link. Please check Spam or Junk folder shortly after registration to make sure. If not, please try using an alternative email address.)

Tentative Agenda: (All Time PDT (GMT -0700))

10:30 am: Check-in, Networking
11:00 am: Introduction and welcome
11:10 am: Presentation + Q/A
12:40 pm: Networking, Adjourn.
02:00 pm: Leave Meeting Room by 2 pm PDT.

Disclaimer: The views of the speakers do not represent the views of AIAA or the AIAA Los Angeles-Las Vegas Section.

Contact: General Contact: contact@aiaa-lalv.org, Events/Program events.aiaalalv@gmail.com

AIAA LA-LV 8/9 Section Aero Alumni (Hybrid) Meeting
Wednesday, August 9, 11 AM - 1 PM PDT (GMT -0700) (US and Canada)

Aero Alumni Meeting

Zoom on-line meeting and in-person as well.

Our monthly Aero Alumni Zoom meeting is at 11 am PDT (on-line and in-person) on August 9 (The 2nd Wednesday of August). It will be a hybrid meeting. "Aero Alumni" are retirees from aerospace industries. All public are welcome to attend. Open to public with free admission. Please Contact [Mr. Gary Moir](mailto:gary.moir@ingenuir.com) for your attendance, on-line or in-person.

In-Person in:
Malibu Library

23519 W CIVIC CENTER WAY MALIBU, CA 90265

*(This meeting is not sponsored by the Malibu Library)
 (South of Hwy 101, North of PCH 1, East of Route 23, and West of Hwy 27)
 (Conveniently located adjacent to the PCH 1 exit at Cross Creek Rd or Webb Way, HRL Laboratories, Pepperdine University (Malibu),
 Frederick R. Weisman Museum of Art, and Our Lady of Malibu Catholic Church)*

In-person attendees are welcome to bring own food / lunch , or order own food / lunch (not through AIAA LA-LV Section). For reference, there Whole Foods close to the library and many restaurants in the Whole Foods shopping center, the Malibu Country Mart, and Malibu Village, etc. No lunch will be provided by the AIAA LA-LV Section.

Online on Zoom:

Join Zoom Meeting: <https://aiaa.zoom.us/j/84036602297?pwd=SUUwdTcyK0diVGxKMHVyaDVhQk9sUT09>

Meeting ID: 840 3660 2297

Passcode: 676619

One tap mobile +16694449171,,84036602297# US, +17193594580,,84036602297# US (Tacoma)

Dial by your location

1 669 444 9171 US

1 719 359 4580 US

1 720 707 2699 US (Denver)

1 253 205 0468 US

1 253 215 8782 US (Tacoma)

1 346 248 7799 US (Houston)

1 305 224 1968 US

1 309 205 3325 US

1 312 626 6799 US (Chicago)

1 360 209 5623 US

1 386 347 5053 US

1 507 473 4847 US

1 564 217 2000 US

1 646 558 8656 US (New York)

1 646 931 3860 US

1 689 278 1000 US

1 301 715 8592 US (Washington DC)

888 475 4499 US Toll-free

877 853 5257 US Toll-free

Meeting ID: 840 3660 2297

+Find your local number: <https://aiaa.zoom.us/j/84036602297?pwd=SUUwdTcyK0diVGxKMHVyaDVhQk9sUT09>

Please contact Mr. Gary Moir (gary.moir@ingenuir.com)

RSVP and Information: (<https://conta.cc/3MtxzJu>)

AIAA LA-LV 8/12 Section Meeting

Saturday, August 12, 11:15 AM PDT (Check-in & Display) / 1 PM PDT (Talk)

The X-15 Rocket Plane, Flying the First Wings into Space by

Ms. Michelle Evans

Author, Bestseller "The X-15 Rocket Plane, Flying the First Wings into Space" Founder and President, Mach 25 Media (www.Mach25Media.com)

AIAA Distinguished Lecturer

Writer, Photographer, and Communications Specialist in aerospace
(The speaker will present in person.)



Location

Michelle Obama Neighborhood Library
5870 Atlantic Ave.

Community Meeting Room
Long Beach, CA 90805

(North East of the Long Beach Airport (LGB), Boeing Long Beach, Relativity Space, and Spinlaunch)
(South of Hwy 91, North of Hwy 405, East of Hwy 710, and West of Hwy 605)
(Library parking entrance from E 59 St behind / on the side of the Library)
(This event is not sponsored by the Michelle Obama Neighborhood Library)

Tentative Agenda: (All Time PDT (GMT -0700)) (US / Canada)

11:00 am: Doors open, setup,
11:15 am: Check-in, Networking, book-signing
12:00 am: Networking, book-signing, and lunch (for who ordered or bring their lunches)
13:00 am: Presentation and Q/A
14:45 pm: Adjourn.
03:00 pm: Meeting Room closes.
(copies of books are available on-site for inscription.)

Disclaimer: The views of the speakers do not represent the views of AIAA or the AIAA Los Angeles-Las Vegas Section.

Contact: General Contact: contact@aiaa-lalv.org, Events/Program events.aiaalalv@gmail.com

RSVP and Information: (<https://conta.cc/3oqK5jp>) (Free Admission, Please RSVP on-line.)

AIAA LA-LV 8/19 Movie Saturday
Saturday, August 19 (US and Canada)

AIAA LA-LV Movie Event

"X-15"

Get ready for an exciting and educational Saturday with some great entertainment and a journey into space! Also enjoy a display of "X-15" movie memorabilia, and more.

Bring the whole family down to enjoy and learn. The X-15 expert, Ms. Michelle Evans, will be there to introduce, comment, and answer questions.

Introduction, Comment, and Q&A by

Ms. Michelle Evans

Author, Bestseller "The X-15 Rocket Plane, Flying the First Wings into

Space" Founder and President, Mach 25 Media (www.Mach25Media.com) AIAA Distinguished Lecturer

Writer, Photographer, and Communications Specialist in aerospace



Before Top Gun, Apollo 13, or The Right Stuff, this breathtaking, jet-fueled journey of high-altitude filmmaking blasted audiences from zero-G to 4,000 miles per hour with its thrilling tale of America's victory in the space race. X-15 sets the sky as the limit for excitement! The courageous pilots of the Air Force's X-15 program are determined to take an experimental rocket plane high above the Earth and into space at six times the speed of sound!

The film stars Charles Bronson and Mary Tyler Moore, and was released in 1961.

In addition to a display, there will be an Introduction prior to the movie, along with Q&A and discussion following the movie.

More movie information: <http://www.mach25media.com/x15movie.html>



Location

Angelo M. Iacoboni Library (Meeting Room)

4990 Clark Ave.,

Lakewood, CA 90712

(North East of the Long Beach Airport (LGB), Boeing Long Beach, Relativity Space, and Spinlaunch)

South of 105/91 Hwy, North of 405 Hwy, East of 710 Hwy, West of 605 Hwy.

(Near Cal State Univ Long Beach and Long Beach Airport (LGB))

(This event is not sponsored by the Angelo M. Iacoboni Library)

(Library Parking is next to the back side of the Library in the Parking Lot. City

Parking is available in the Parking Lot. Please follow the signs for either.)

Tentative Agenda: (All Time PDT (GMT -0700)) (US / Canada)

11 AM Check-in, Displays

1 PM PDT Movie

3 PM PDT Rerun

(No lunch will be provided. You are welcome to bring your own food. No alcoholic beverages or food in the library.)

Disclaimer: The views of the speakers do not represent the views of AIAA or the AIAA Los Angeles-Las Vegas Section.

Contact: General Contact: contact@aiaa-lalv.org, Events/Program events.aiaalav@gmail.com